

**Engineering Sciences**

**MAY 1 '75**

**Branch Library**

**WIND-ENGINEERING STUDY OF  
UNIVERSITY OF PENNSYLVANIA HOSPITAL**

by

**J. A. Peterka\* and J. E. Cermak\*\***

for

**Skilling, Helle, Christiansen and Robertson  
230 Park Avenue  
New York, N. Y. 10017**

**Fluid Mechanics and Wind Engineering Program  
Fluid Dynamics and Diffusion Laboratory  
Department of Civil Engineering  
Colorado State University  
Fort Collins, Colorado  
March 1975**

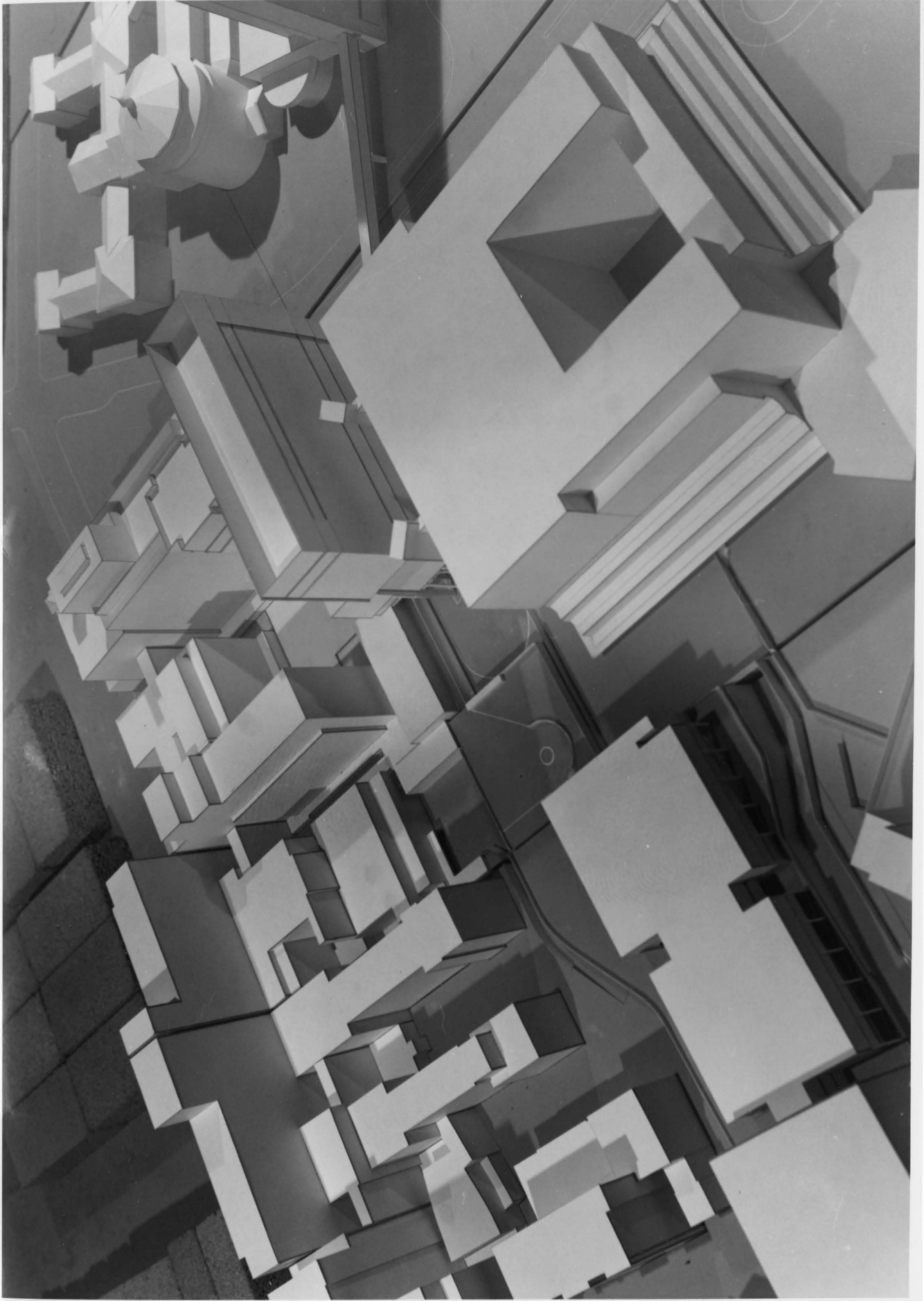


**U18401 0074158**

**\* Assistant Professor**

**\*\* Professor-in-Charge, Fluid Mechanics and Wind Engineering Program**

**CER74-75JAP-JEC36**



UNIVERSITY OF PENNSYLVANIA HOSPITAL  
(1:240 Scale Model)

## TABLE OF CONTENTS

<u>Chapter</u>		<u>Page</u>
	ACKNOWLEDGMENTS . . . . .	iii
	LIST OF TABLES . . . . .	iv
	LIST OF FIGURES . . . . .	v
	LIST OF SYMBOLS . . . . .	vii
I	INTRODUCTION . . . . .	1
	1.1 General . . . . .	1
	1.2 The University of Pennsylvania Hospital . . . . .	2
II	EXPERIMENTAL CONFIGURATION . . . . .	3
	2.1 Wind Tunnel . . . . .	3
	2.2 Model . . . . .	3
III	INSTRUMENTATION AND DATA ACQUISITION . . . . .	5
	3.1 Flow Visualization . . . . .	5
	3.2 Velocity . . . . .	5
	3.3 Pressure . . . . .	7
IV	RESULTS . . . . .	8
	4.1 Flow Visualization . . . . .	8
	4.2 Velocity . . . . .	9
	4.3 Pressure . . . . .	11
V	CONCLUSIONS . . . . .	12
	REFERENCES . . . . .	13
	TABLES . . . . .	14
	FIGURES . . . . .	28

## ACKNOWLEDGMENTS

Support for this investigation was provided by Skilling, Helle, Christiansen and Robertson and Westermann Miller Associates. The architect's model used in the study was supplied by Westermann Miller Associates. Mr. J. Maxton was responsible for photography and Mr. G. L. Marsh was responsible for velocity data acquisition.

LIST OF TABLES

<u>Table</u>		<u>Page</u>
1	MOTION PICTURE SCENE GUIDE . . . . .	14
2	MEAN AND FLUCTUATING VELOCITIES IN PEDESTRIAN AREAS . . . . .	15
3	PRESSURE DATA . . . . .	27

## LIST OF FIGURES

<u>Figure</u>		<u>Page</u>
1	Environmental Wind Tunnel . . . . .	28
2	Model Configurations . . . . .	29
3	Model Installed in Wind Tunnel . . . . .	31
4	Velocity Measurement and Gas Discharge Locations . . . . .	32
5	Pressure Tap Locations . . . . .	33
6	Flow Visualization Using Smoke . . . . .	34
7	Typical Hot-Wire Calibration . . . . .	35
8	Mean Velocity Profiles Approaching the Model . . . .	36
9	Turbulence Intensity Profiles . . . . .	38
10	Mean Velocity and Turbulence Intensity at Point 1 . .	39
11	Mean Velocity and Turbulence Intensity at Point 2 . .	40
12	Mean Velocity and Turbulence Intensity at Point 3 . .	41
13	Mean Velocity and Turbulence Intensity at Point 4 . .	42
14	Mean Velocity and Turbulence Intensity at Point 5 . .	43
15	Mean Velocity and Turbulence Intensity at Point 6 . .	44
16	Mean Velocity and Turbulence Intensity at Point 7 . .	45
17	Mean Velocity and Turbulence Intensity at Point 8 . .	46
18	Mean Velocity and Turbulence Intensity at Point 9 . .	47
19	Mean Velocity and Turbulence Intensity at Point 10. .	48
20	Mean Velocity and Turbulence Intensity at Point 11. .	49
21	Mean Velocity and Turbulence Intensity at Point 12. .	50
22	Mean Velocity and Turbulence Intensity at Point 13. .	51
23	Mean Velocity and Turbulence Intensity at Point 14. .	52
24	Mean Velocity and Turbulence Intensity at Point 15. .	53

<u>Figure</u>		<u>Page</u>
25	Mean Velocity and Turbulence Intensity at Point 16. .	54
26	Mean Velocity and Turbulence Intensity at Point 17. .	55
27	Mean Velocity and Turbulence Intensity at Point 18. .	56
28	Mean Velocity and Turbulence Intensity at Point 19. .	57

## LIST OF SYMBOLS

<u>Symbol</u>	<u>Definition</u>
U	Local mean velocity
D	Characteristic dimension (building height, width, etc.)
$\nu$	Kinematic viscosity of approach flow
$\frac{UD}{\nu}$	Reynolds number
E	Mean voltage
A	Constant
B	Constant
n	Constant
$U_{rms}$	Root-mean-square of fluctuating velocity
$E_{rms}$	Root-mean-square of fluctuating voltage
$U_{\infty}$	Reference mean velocity outside the boundary layer
Y	Height above surface
$\delta$	Height of boundary layer
$T_u$	Turbulence intensity $U_{rms}/U_{\infty}$
$C_{p_{mean}}$	Mean pressure coefficient, $\frac{(p-p_{\infty})_{mean}}{\frac{1}{2} \rho U_{\infty}^2}$
$\rho$	Density of approach flow
p	Pressure at a pressure tap on the structure
$p_{\infty}$	Static pressure in the wind tunnel above the model

## 1. INTRODUCTION

### 1.1 General

Increased use of pedestrian plaza areas in modern architectural design has brought about a greater need to consider wind and gustiness in the design of these areas. Recognition that tall buildings generate winds in pedestrian areas about the structure has led to increased concern about the effects of a proposed structure on the wind environment in pedestrian areas. Because nearby buildings may also affect local wind characteristics, the architect may want to consider these influences in the placement and design of building entrances or plazas. Techniques have been developed during the past decade for wind-tunnel modeling of atmospheric winds about building complexes which allow the prediction of the wind environment near the buildings. This information permits pedestrian areas to be protected by design changes before the building is constructed or, if construction is complete, permits an evaluation of possible measures under consideration for alleviation of wind problems.

Modeling the atmospheric winds about a structure requires special consideration of flow conditions in order to guarantee similitude between model and prototype. A detailed discussion of the similarity requirements and their wind-tunnel implementation can be found in References [1], [2], and [3]. In general, the requirements are that the model and prototype be scaled in geometry, that the approach mean velocity at the building site have a vertical profile shape similar to the full-scale flow, that the turbulence characteristics of the flows be similar, and that the Reynolds number for the model and prototype be equal.

These criteria are satisfied by constructing a scale model of the structure and its surroundings and performing the wind tests in a wind tunnel specifically designed to model atmospheric boundary-layer flows. Reynolds number similarity requires that the quantity  $UD/\nu$  be similar for model and prototype. Since  $\nu$ , the kinematic viscosity of air, is identical for both, Reynolds numbers cannot be made equal with reasonable wind velocities. Wind velocity in the wind tunnel would have to be the model scale factor times the prototype wind. However, for sufficiently high Reynolds number ( $>10^5$ ) a pressure coefficient at any location on the structure will be essentially constant with Reynolds number. Typical values encountered are  $10^8$  for the full scale and  $10^6$  for the wind-tunnel model. Thus acceptable flow similarity is achieved without precise Reynolds number equality.

## 1.2 The University of Pennsylvania Hospital

A wind-engineering study was performed for the University of Pennsylvania Hospital addition, Phase III, proposed Silverstein building and Medical Education complex. A 1:240 scale architect's model (frontispiece) was used. The objectives of the wind-engineering study were to obtain wind velocity and gustiness in pedestrian areas about the structure and to obtain pressures at two points on the structure. In addition, a flow-visualization study was performed to define overall flow patterns and determine regions of possible pedestrian discomfort.

## 2. EXPERIMENTAL CONFIGURATION

### 2.1 Wind Tunnel

The wind-engineering study was performed in the environmental wind tunnel located in the Fluid Dynamics and Diffusion Laboratory at Colorado State University, Figure 1. The tunnel is an open-circuit facility driven by a 15 h.p. variable-pitch propeller. The test section is nominally 12 ft wide, 8 ft high and 52 ft long fed through a 3.35:1 contraction ratio. The roof is adjustable to maintain a zero pressure gradient along the test section. The mean velocity can be adjusted continuously from 1 to 20 fps.

### 2.2 Model

A 1:240 scale architect's model supplied by Westermann Miller Associates was used for the wind-tunnel tests. Three configurations of the model were used, Figure 2. Configuration A represented the pre-construction geometry without the Silverstein or Medical Education buildings. Configuration B added the Silverstein building and a low-level Medical Education building. Configuration C included the Silverstein building with a taller Medical Education building.

The model was installed on the 12 ft-diameter turntable located 25 ft from the test-section entrance. An area of 1400 ft radius surrounding the model center was modeled to simulate general building shape and height. The region upstream from the modeled area was covered with a randomized roughness constructed from 1 in. cubes. A spire arrangement at the test-section entrance provided a thicker boundary layer than would otherwise be available. The upstream configuration was designed to provide approximately a 2 ft boundary-layer thickness, a velocity power law appropriate to the University of Pennsylvania

Hospital site, and a logarithmic velocity profile with a realistic roughness length. A photograph of the model installed in the wind tunnel is shown in Figure 3.

Eight locations on the model were selected for quantitative velocity measurements. These locations are shown in Figure 4. These locations were selected in conjunction with Skilling, Helle, Christiansen and Robertson and the Architect to provide maximum information regarding pedestrian comfort levels in the primary pedestrian areas.

Two pressure taps were installed on the Silverstein building--one at each end. The purpose was to provide an indication of pressure differential across the building which could be used to determine approximate flow magnitudes through the pedestrian and auto passages under the Silverstein building. The pressure taps were located symmetrically--one at each end of the structure--in the position shown by the arrow in Figure 5.

### 3. INSTRUMENTATION AND DATA ACQUISITION

#### 3.1 Flow Visualization

Visualization of the flow in the vicinity of the model is helpful in locating regions of high velocity or gustiness. It is also useful in indicating where exhausts from cooling towers or underground parking areas will be transported by the winds. Titanium-tetrachloride smoke was released from sources on and near the model as shown in Figure 7 and motion picture records made. Conclusions obtained from these smoke studies are discussed in Section 4.1.

#### 3.2 Velocity

Vertical velocity and turbulence-intensity profiles were measured upstream of the model and at the Silverstein building location for model Configuration A. In addition, mean velocity and turbulence-intensity measurements were made 0.3 in. (6.0 ft) above the surface at the eight locations indicated in Figure 4 for three model configurations at 24 wind directions. The surface measurements are indicative of the environment to which a pedestrian in the plaza area would be subjected. The eight surface locations in Figure 4 have numbers from 1 to 19 associated with them. Numbers 1 to 8 indicate the eight positions for model Configuration A, numbers 9 to 16 indicate the same eight positions for model Configuration B, and numbers 17 to 19 indicate the three locations near the Medical Education building for model Configuration C. Elevations are given by each data location to indicate the surface elevation at each location where measurements were taken. Since no structure was in place for data locations 5 and 8 (Configuration A) which are indicated at 52 ft elevation, these two points were taken 6 ft above the existing ground level in Configuration A.

Measurement of velocity at each location was made with a single hot-wire anemometer mounted with its axis vertical. The instrumentation used was a Thermo-Systems constant temperature anemometer (Model 1050) with a 0.001 in. dia. platinum-film sensing element 0.020 in. long. Output was read from a Hewlett-Packard integrating digital voltmeter for mean voltage and a DISA RMS meter for rms voltage.

Calibration of the hot-wire anemometer was performed using a Thermo-Systems Calibrator (Model 1125). The calibration data was fit to a variable exponent King's-law relationship

$$E^2 = A + BU^n$$

where  $E$  is the hot-wire output voltage,  $U$  the approach velocity and  $A$ ,  $B$  and  $n$  are coefficients selected to fit the calibration data. A typical calibration showing the linear relationship between  $E^2$  and  $U^n$  is plotted in Figure 7. The above relationship was used to recover the mean velocity at measurement points from the measured mean voltage. The fluctuating velocity in the form  $U_{rms}$  (root-mean-square velocity) was obtained from

$$U_{rms} = \frac{2 E E_{rms}}{B n U^{n-1}}$$

where  $E_{rms}$  is the root-mean-square voltage output from the anemometer. All turbulence velocities were divided by both local mean velocity  $U$  and mean velocity outside the boundary layer  $U_\infty$ . Division by  $U$  gives an indication of the relative unsteadiness at the location while division by  $U_\infty$  permits easy determination of the actual magnitude of rms velocity fluctuations at a point for various approach velocities.

### 3.3 Pressure

Mean pressures were obtained at the two pressure tap locations described in Section 2.2. The two pressure taps were designated as the East Tap,  $P_1$ , located at the east end of the Silverstein building and as the West Tap,  $P_2$ , located at the west end of the building. The pressures at each tap were measured at each of the 24 wind directions for which velocity measurements were made. Each pressure measurement was recorded as a pressure coefficient defined as

$$C_{P_{\text{mean}}} = \frac{(p - p_{\infty})_{\text{mean}}}{\rho U_{\infty}^2 / 2}$$

where  $p$  is the local pressure at pressure tap locations  $P_1$  or  $P_2$  on the structure,  $p_{\infty}$  is the static pressure in the wind tunnel above the model at the edge of the boundary layer,  $( )_{\text{mean}}$  indicates the mean of the pressure difference, and  $\rho U_{\infty}^2 / 2$  is the dynamic pressure associated with the velocity  $U_{\infty}$  at the edge of the boundary layer. The pressure difference  $(p - p_{\infty})$  was measured directly with an MKS Baratron differential pressure sensor.

Since the difference in pressure between the two taps was of interest, the difference in pressure between the two taps was also measured directly. These data are presented in the form

$$\Delta C_{P_{\text{mean}}} = \frac{(p_1 - p_2)_{\text{mean}}}{\rho U_{\infty}^2 / 2}$$

where  $p_1$  and  $p_2$  are the pressures at taps  $P_1$  and  $P_2$ . Conversion of the pressure coefficients into full scale pressures is accomplished by multiplying the coefficient by the full scale dynamic pressure  $\rho U_{\infty}^2 / 2$  associated with any desired prototype wind magnitude.

## 4. RESULTS

### 4.1 Flow Visualization

A 450 ft film is included as part of this report showing characteristics of flow about the model using smoke to make the flow visible. A listing of the contents of the film is shown in Table 1. Smoke was released at a number of points on the model in pedestrian areas and at points of cooling-tower exhaust or other roof discharges. Smoke flow was photographed for each of the three configurations at each of four wind directions--North, Southeast, Southwest and West. In addition, the flow in the pedestrian area between the Silverstein and Medical Education buildings (velocity location 19) was examined at 15 degree wind direction intervals from Southeast through Southwest for Configuration C. A 10 ft wind screen with 50 percent porosity was added to show the effect of the screen. For several wind directions, a 20 ft wind screen was used in addition. Several conclusions were evident from the flow visualization.

The wind velocities were moderate to low in all pedestrian areas for all wind directions investigated for Configurations B and C. Velocities were generally lower than for Configuration A--the before-construction configuration. Flow was observed under the Silverstein building for some wind directions; however, the major part of the flow passed between the Silverstein and Chop buildings. For southerly winds (Southeast to Southwest) a strong wind flow was observed between the Medical Education and Chop buildings which resulted in moderately strong winds in the region of velocity measurement point 19. A 10 ft fence with 50 percent porosity at the southern edge of that pedestrian plaza appeared to decrease winds at point 19 somewhat while a 20 ft fence made a more significant improvement.

Smoke releases from cooling towers and other roof discharges showed a rapid dispersion of vented material. Impingement of these sources on the Silverstein building covered a wide area of the structure. Smoke release from the pathological burner outlet on top of the Medical Education building showed a rapid dispersal over a wide area with no tendency to concentrate in any one location.

#### 4.2 Velocity

Approach velocity profiles are shown in Figures 8a and 8b. These profiles were taken upstream from the model representing the characteristics of the boundary layer approaching the model and the flow characteristics at the Silverstein building site for Configuration A. The boundary-layer thickness,  $\delta$ , was 24 in. corresponding to a prototype value of 384 ft. Although the boundary-layer thickness is somewhat smaller than anticipated for the field site, this should cause little influence on the velocities within the model which are dominated by building wake flows. In the form

$$\frac{U}{U_{\infty}} = \left(\frac{y}{\delta}\right)^n$$

the velocity profile has an exponent  $n$  of 0.3 for the approach flow which is an acceptable value for city environments such as Philadelphia with moderate building heights extending for a distance outward from the building site. The effects of the surrounding hospital buildings on the approach flow can be seen in the profile obtained at the building location. The profile plotted in Figure 8b is shown in semilogarithmic form to display the effective roughness length. The effective roughness height  $Y_0$  indicated by the zero velocity intercept of the best fit line is 6.4 ft, which is slightly large but not unreasonable for the site modeled.

Profiles of longitudinal turbulence intensity are shown in Figure 9 for both the upstream and model-removed conditions. Modifications to the profiles due to structures located upwind are evident. For the purpose of this report, turbulence intensity is defined as the root-mean-square of the longitudinal velocity fluctuations divided by the reference mean velocity  $U_{\infty}$  at the outer edge of the boundary layer,

$$Tu_1 = \frac{U_{rms}}{U_{\infty}},$$

or as the rms velocity divided by the local mean velocity,

$$Tu_2 = \frac{U_{rms}}{U}.$$

Mean velocity and turbulence intensity at locations 1-19 shown in Figure 4 for 24 wind directions are listed in Table 2 and are plotted in Figures 10-28. Measurements were taken 0.3 in. (6.0 ft prototype) above the surface. A site map is superimposed on the polar plots to aid in visualization of the effects of nearby structures on the results.

The largest velocities were measured at points 7 and 8 (Configuration A without the new buildings) for wind directions of 60 and 45 degrees at 63 and 58 percent of the reference velocity  $U_{\infty}$ . With the new buildings in place, the largest velocity was located at point 16 for a 45 degree wind azimuth at 47 percent of  $U_{\infty}$ . Most mean velocities were significantly below this level. The largest value of rms velocity was 17 percent of  $U_{\infty}$  found at points 15 and 16 for wind directions of 60 and 45 degrees. Numerous other points had values in the 13 to 16 percent region. The largest values of "gustiness" or

local turbulence intensity ( $U_{\text{rms}}/U$ ) were in the range of 50 to 58 percent found at a number of locations. Large values of gustiness must be interpreted in terms of the magnitude of mean velocity since a low local wind velocity can lead to large values as effectively as large rms velocities.

#### 4.3 Pressure

The pressures measured at pressure taps  $P_1$  and  $P_2$  are listed in Table 3 along with the measured difference in pressure between the two pressure taps. An indication of the accuracy of measurement can be obtained by comparing the difference between the mean  $C_p$  values for the individual taps and the  $\Delta C_p$  values measured directly. The agreement is good. The largest pressure difference across the building is approximately 0.35--a reasonable value for pressure taps located low on a building surrounded by buildings of comparable height.

## 5. CONCLUSIONS

A simulated atmospheric boundary-layer flow over the University of Pennsylvania Hospital model was established to examine the wind characteristics in pedestrian areas about the proposed addition consisting of the Silverstein building and two configurations of the Medical Education building. Smoke was released at numerous locations about the model for several wind directions to determine qualitatively the wind characteristics in pedestrian areas, to determine how quickly the exhausts from nearby roof vents dispersed, and to determine whether significant impingement occurred on the proposed buildings. Quantitative measurements of wind velocity and turbulence were obtained at selected locations for 24 wind directions to determine areas where pedestrian comfort might be a problem.

The results from both smoke flow and quantitative velocity measurements indicated that the addition of the Silverstein and Medical Education buildings to the complex caused no adverse effects to the winds in the pedestrian areas about the buildings. The winds were, in general, lower with the addition of the structures than in the before-construction configuration. The effects of the addition of a 10 ft or 20 ft porous wind screen across the southern edge of the pedestrian area between the Silverstein and Medical Education building to protect against southerly winds were determined by visualization with smoke flow. The results indicated increasing improvement in wind characteristics in the pedestrian area with increased height of fence.

## REFERENCES

1. Davenport, A. G. and N. Isyumov, "The application of the boundary layer wind tunnel to the prediction of wind loading," Proc. of Int. Res. Seminar on Wind Effects on Buildings and Structures, VI, N.R.C., Canada, 1967.
2. Cermak, J. E., "Laboratory simulation of the atmospheric boundary layer," AIAA J1., V9, Sept. 1971.
3. Cermak, J. E., "Applications of fluid mechanics to wind engineering--A Freeman Scholar Lecture," ASME J1. of Fluids Engineering, Vol. 97, Series 1, No. 1, March 1975.

TABLE 1  
MOTION PICTURE SCENE GUIDE  
UNIVERSITY OF PENNSYLVANIA HOSPITAL

SCENE	MODEL CONFIGURATION	WIND AZIMUTH	WIND VELOCITY, FPS
Titles			
Wind Tunnel and Model Installation			
Run 1	A	N	10
2	A	SE	"
3	A	SW	"
4	A	W	"
5	B	N	"
6	C	N	"
7	B	SE	"
8	C	SE	"
9	B	SW*	"
10	C	SW	"
11	B	W	"
12	C	W	"
13	B	SE-SW**	"

\* Wind-direction arrow in movie indicates incorrect direction.

\*\* Wind arrow indicates approach wind direction.  
10 ft wind screen used for all wind directions.  
20 ft wind screen used for several wind directions.

TABLE 2  
MEAN AND FLUCTUATING VELOCITIES IN PEDESTRIAN AREAS

WIND AZIMUTH (degrees)	MEASUREMENT LOCATION	$U/U_{\infty}$ (percent)	$U_{rms}/U_{\infty}$ (percent)	$U_{rms}/U$ (percent)
0	1	22.8	7.3	32.2
	2	11.7	6.0	51.3
	3	23.3	9.0	38.5
	4	27.2	8.5	31.3
	5	28.9	9.5	33.0
	6	22.2	7.7	34.5
	7	27.3	6.5	23.7
	8	29.4	9.3	31.8
	9	18.6	8.2	44.0
	10	19.5	6.5	33.4
	11	20.2	6.7	33.2
	12	5.6	2.1	37.6
	13	3.1	.6	19.9
	14	4.5	1.1	25.7
	15	26.3	6.1	23.3
	16	20.3	8.8	43.1
	17	12.9	5.3	41.3
	18	13.7	5.0	36.7
	19	16.4	5.9	35.8
15	1	23.0	8.7	37.8
	2	13.3	6.5	49.1
	3	21.2	8.5	40.3
	4	30.0	10.2	34.0
	5	34.7	10.9	31.4
	6	28.2	9.0	32.1
	7	24.5	9.4	38.4
	8	36.7	7.4	20.3
	9	9.6	4.4	46.3
	10	24.0	8.2	34.1
	11	21.9	8.2	37.4
	12	8.5	3.7	44.2
	13	3.1	.7	22.4
	14	4.3	1.3	29.1
	15	33.4	6.2	18.6
	16	27.7	13.4	48.3
	17	18.1	6.7	36.8
	18	18.3	5.8	31.8
	19	18.3	7.2	39.5

TABLE 2 (continued)

WIND AZIMUTH (degrees)	MEASUREMENT LOCATION	$U/U_{\infty}$ (percent)	$U_{rms}/U_{\infty}$ (percent)	$U_{rms}/U$ (percent)
30	1	14.4	4.5	31.1
	2	17.4	7.2	41.6
	3	22.3	8.3	37.3
	4	28.9	10.9	37.7
	5	35.2	10.9	31.1
	6	25.4	10.5	41.4
	7	32.7	10.9	33.5
	8	44.2	7.2	16.3
	9	12.2	5.5	45.1
	10	22.3	8.3	37.0
	11	18.5	7.5	40.5
	12	7.2	2.8	38.8
	13	4.2	.9	20.6
	14	5.4	1.8	33.2
	15	29.7	7.2	24.1
	16	35.8	14.7	41.0
	17	12.5	4.1	33.1
	18	17.4	6.1	34.9
	19	15.2	6.7	43.9
45	1	14.3	5.3	36.8
	2	21.9	10.2	46.5
	3	24.9	10.0	40.3
	4	26.8	12.9	48.1
	5	42.2	12.6	29.9
	6	20.1	11.5	57.2
	7	44.9	15.0	33.4
	8	58.0	8.8	15.1
	9	15.5	5.9	38.0
	10	21.5	7.6	35.2
	11	15.5	5.8	37.2
	12	9.1	4.3	47.5
	13	2.9	.5	17.9
	14	6.1	2.2	36.6
	15	43.2	9.2	21.3
	16	46.5	17.0	36.6
	17	9.3	3.1	33.2
	18	16.0	5.5	34.5
	19	13.2	5.6	42.4

TABLE 2 (continued)

WIND AZIMUTH (degrees)	MEASUREMENT LOCATION	$U/U_{\infty}$ (percent)	$U_{rms}/U_{\infty}$ (percent)	$U_{rms}/U$ (percent)
60	1	22.4	7.7	34.3
	2	29.3	10.5	35.7
	3	24.5	11.2	45.9
	4	41.4	12.7	30.8
	5	49.3	12.9	26.2
	6	20.2	11.8	58.1
	7	63.4	8.4	13.3
	8	55.1	9.6	17.5
	9	13.9	5.8	41.9
	10	24.2	10.2	42.1
	11	22.7	9.3	41.0
	12	4.4	1.3	30.5
	13	3.9	1.4	34.7
	14	5.8	2.2	38.0
	15	42.3	8.1	19.0
	16	42.1	17.4	41.4
	17	19.2	7.4	38.5
	18	24.4	8.9	36.6
	19	19.6	8.1	41.4
75	1	20.6	8.1	39.2
	2	21.9	9.0	41.1
	3	19.3	9.5	49.1
	4	29.7	12.4	41.8
	5	38.5	12.3	31.9
	6	31.1	14.7	47.1
	7	59.4	11.2	18.8
	8	51.3	10.8	21.0
	9	18.5	9.6	52.0
	10	14.2	7.0	49.7
	11	14.3	7.8	54.8
	12	3.8	1.0	26.1
	13	4.5	1.9	42.8
	14	6.1	2.2	36.7
	15	39.3	11.1	28.3
	16	33.3	15.5	46.5
	17	19.9	6.6	33.3
	18	29.3	10.2	35.0
	19	18.1	7.7	42.3

TABLE 2 (continued)

WIND AZIMUTH (degrees)	MEASUREMENT LOCATION	$U/U_{\infty}$ (percent)	$U_{\text{rms}}/U_{\infty}$ (percent)	$U_{\text{rms}}/U$ (percent)
90	1	25.2	8.4	33.3
	2	23.3	11.5	49.5
	3	24.1	8.5	35.4
	4	38.5	9.4	24.4
	5	43.4	9.1	21.0
	6	41.3	9.2	22.2
	7	40.6	10.0	24.7
	8	32.4	10.8	33.2
	9	11.2	5.1	45.4
	10	9.0	3.6	40.5
	11	10.7	4.6	43.1
	12	3.9	1.0	24.4
	13	13.5	4.7	34.9
	14	11.9	4.8	40.3
	15	24.6	7.8	31.8
	16	41.8	17.8	42.6
	17	11.6	4.7	40.9
	18	14.0	3.3	23.8
	19	12.1	5.8	47.5
105	1	35.7	14.9	41.7
	2	10.4	5.9	56.1
	3	17.0	8.2	48.2
	4	32.4	11.9	36.7
	5	36.3	11.6	32.0
	6	39.9	12.0	30.2
	7	44.8	14.5	32.3
	8	32.4	14.3	44.2
	9	26.8	10.3	38.3
	10	7.2	2.4	33.2
	11	8.4	2.7	32.2
	12	6.0	2.1	34.8
	13	20.1	5.8	29.0
	14	20.2	5.9	29.2
	15	25.9	10.7	41.5
	16	14.5	6.9	47.7
	17	30.7	7.4	24.2
	18	8.9	1.9	21.0
	19	5.6	2.1	38.1

TABLE 2 (continued)

WIND AZIMUTH (degrees)	MEASUREMENT LOCATION	$U/U_{\infty}$ (percent)	$U_{\text{rms}}/U_{\infty}$ (percent)	$U_{\text{rms}}/U$ (percent)
120	1	13.4	6.3	46.8
	2	8.8	3.9	45.0
	3	22.2	8.4	37.7
	4	43.7	9.5	21.7
	5	47.8	9.8	20.6
	6	45.0	9.0	19.9
	7	19.6	8.8	44.7
	8	13.7	7.3	53.0
	9	26.3	9.6	36.6
	10	6.6	2.2	33.7
	11	6.8	2.4	35.3
	12	7.6	3.2	42.1
	13	24.5	6.7	27.2
	14	24.7	5.1	20.6
	15	12.9	5.8	45.1
	16	10.4	4.1	39.2
	17	31.5	5.8	18.5
	18	10.9	5.5	50.5
	19	16.8	7.0	41.8
135	1	14.4	6.9	47.7
	2	9.5	4.4	45.9
	3	23.9	8.7	36.6
	4	46.4	10.0	21.7
	5	47.7	9.4	19.6
	6	43.6	8.9	20.4
	7	17.9	8.0	45.0
	8	13.7	6.9	50.6
	9	16.7	8.4	50.5
	10	8.0	2.9	36.0
	11	8.4	3.1	36.8
	12	7.2	2.7	37.9
	13	28.0	6.9	24.5
	14	26.7	8.2	30.9
	15	11.1	5.2	47.5
	16	11.6	4.1	35.5
	17	33.7	6.5	19.4
	18	10.4	5.1	48.9
	19	15.4	7.2	46.6

TABLE 2 (continued)

WIND AZIMUTH (degrees)	MEASUREMENT LOCATION	$U/U_{\infty}$ (percent)	$U_{rms}/U_{\infty}$ (percent)	$U_{rms}/U$ (percent)
150	1	24.7	10.8	43.7
	2	10.5	4.7	45.0
	3	22.2	9.0	40.5
	4	44.9	10.7	23.8
	5	47.6	9.5	20.1
	6	46.3	8.0	17.2
	7	18.6	8.0	43.2
	8	12.9	6.3	48.4
	9	17.4	8.0	46.0
	10	5.9	1.9	32.3
	11	6.1	2.2	36.2
	12	8.5	3.5	41.0
	13	27.2	6.3	23.0
	14	23.8	9.1	38.4
	15	12.3	5.4	44.0
	16	13.1	1.5	11.7
	17	33.6	6.0	17.9
	18	25.0	14.5	58.0
	19	32.8	10.1	30.7
165	1	20.6	7.9	38.3
	2	9.6	4.8	49.5
	3	11.0	5.1	45.8
	4	38.3	10.8	28.3
	5	37.8	11.0	29.0
	6	42.1	8.3	19.7
	7	18.6	8.8	47.2
	8	12.2	5.7	47.0
	9	15.7	7.1	45.2
	10	9.2	3.2	34.8
	11	12.3	5.8	47.3
	12	15.5	6.9	44.9
	13	27.5	5.1	18.7
	14	16.8	7.9	47.2
	15	20.4	9.9	48.6
	16	18.8	7.7	41.2
	17	26.4	8.0	30.4
	18	7.3	2.7	37.0
	19	20.5	10.0	48.8

TABLE 2 (continued)

WIND AZIMUTH (degrees)	MEASUREMENT LOCATION	$U/U_{\infty}$ (percent)	$U_{rms}/U_{\infty}$ (percent)	$U_{rms}/U$ (percent)
180	1	15.9	6.0	37.5
	2	8.8	4.1	46.5
	3	12.8	6.7	52.1
	4	19.0	7.6	39.9
	5	13.1	6.1	46.4
	6	20.5	8.0	38.9
	7	22.7	9.1	40.3
	8	15.2	8.3	54.2
	9	11.7	5.5	47.0
	10	8.0	2.8	35.5
	11	8.0	3.7	46.1
	12	31.6	8.1	25.5
	13	20.3	4.2	20.9
	14	10.7	5.3	49.5
	15	27.6	11.7	42.2
	16	24.8	10.0	40.4
	17	24.2	8.0	33.0
	18	6.9	1.9	28.3
	19	11.9	5.8	48.8
195	1	15.2	6.8	44.8
	2	9.9	4.8	48.1
	3	12.0	6.2	51.9
	4	28.9	8.5	29.3
	5	28.2	8.6	30.6
	6	21.5	7.8	36.1
	7	22.9	7.0	30.6
	8	16.0	8.5	53.3
	9	11.0	4.4	39.8
	10	8.0	2.6	32.2
	11	8.1	3.2	39.3
	12	30.7	7.9	25.7
	13	11.9	3.7	31.3
	14	18.8	8.5	44.9
	15	28.8	13.2	45.8
	16	27.7	10.9	39.6
	17	21.9	7.0	32.2
	18	11.7	2.5	20.9
	19	9.6	3.6	37.9

TABLE 2 (continued)

WIND AZIMUTH (degrees)	MEASUREMENT LOCATION	$U/U_{\infty}$ (percent)	$U_{\text{rms}}/U_{\infty}$ (percent)	$U_{\text{rms}}/U$ (percent)
210	1	13.7	6.3	46.0
	2	11.5	5.8	50.8
	3	29.1	8.4	28.8
	4	35.5	8.2	23.2
	5	43.0	8.0	18.6
	6	28.0	6.8	24.3
	7	27.6	7.6	27.6
	8	22.1	13.1	59.2
	9	23.4	6.7	28.6
	10	8.2	3.1	38.0
	11	13.1	4.6	34.9
	12	27.2	6.0	22.1
	13	10.7	3.6	33.5
	14	18.9	9.3	49.0
	15	23.6	12.0	50.6
	16	29.8	10.9	36.5
	17	18.2	6.0	32.9
	18	18.2	3.8	20.7
	19	16.2	4.4	27.4
225	1	11.7	4.7	40.4
	2	13.5	6.6	48.7
	3	24.0	9.3	38.6
	4	34.8	8.7	24.9
	5	32.9	8.3	25.3
	6	31.9	7.5	23.7
	7	29.0	8.8	30.3
	8	19.1	9.0	47.0
	9	15.1	4.5	29.6
	10	7.7	2.6	33.2
	11	11.6	3.7	31.8
	12	14.9	5.0	33.4
	13	6.9	2.4	34.7
	14	19.9	8.8	44.1
	15	17.7	9.2	52.1
	16	38.3	13.0	33.9
	17	13.4	4.0	29.6
	18	15.1	2.6	17.4
	19	12.4	3.9	31.4

TABLE 2 (continued)

WIND AZIMUTH (degrees)	MEASUREMENT LOCATION	$U/U_{\infty}$ (percent)	$U_{rms}/U_{\infty}$ (percent)	$U_{rms}/U$ (percent)
240	1	10.3	4.9	47.3
	2	12.5	6.3	50.3
	3	13.6	7.2	52.7
	4	38.4	8.5	22.3
	5	32.9	9.3	28.2
	6	25.3	8.4	33.3
	7	29.4	7.2	24.6
	8	18.1	8.2	45.2
	9	14.0	5.1	36.3
	10	7.6	2.7	36.2
	11	11.7	4.1	34.8
	12	7.9	3.6	45.1
	13	7.3	2.8	38.7
	14	18.3	6.1	33.5
	15	17.2	8.4	49.0
	16	26.4	11.3	42.7
	17	11.2	4.1	36.3
	18	14.6	3.2	21.6
	19	12.1	3.8	31.0
255	1	9.7	4.6	46.9
	2	18.1	8.9	49.4
	3	20.5	10.7	52.2
	4	41.4	11.7	28.2
	5	27.6	12.9	46.7
	6	18.4	8.8	47.7
	7	19.0	6.7	35.3
	8	15.2	7.7	50.8
	9	12.8	5.3	41.2
	10	8.3	2.7	32.0
	11	13.8	4.1	29.6
	12	6.8	2.8	40.7
	13	6.6	2.6	40.1
	14	11.4	3.5	31.0
	15	13.5	6.4	47.2
	16	21.6	10.0	46.2
	17	11.2	4.1	36.9
	18	13.8	3.1	22.4
	19	11.4	3.9	34.5

TABLE 2 (continued)

WIND AZIMUTH (degrees)	MEASUREMENT LOCATION	$U/U_{\infty}$ (percent)	$U_{rms}/U_{\infty}$ (percent)	$U_{rms}/U$ (percent)
270	1	12.7	4.8	38.2
	2	11.5	5.6	48.5
	3	12.6	6.7	53.0
	4	15.6	5.9	38.0
	5	15.2	6.2	40.5
	6	9.6	4.5	47.3
	7	14.2	4.9	34.2
	8	15.7	7.6	48.6
	9	10.0	4.1	40.4
	10	6.1	2.0	32.0
	11	7.2	2.9	40.2
	12	10.0	3.4	34.3
	13	16.1	4.0	24.7
	14	23.5	4.4	18.9
	15	14.5	6.7	46.3
	16	16.2	7.3	45.2
	17	12.1	4.9	40.6
	18	15.4	4.4	28.5
	19	14.4	4.5	31.2
285	1	15.9	6.4	40.5
	2	11.5	5.1	44.0
	3	12.6	5.6	44.2
	4	19.5	7.0	35.9
	5	22.6	7.0	31.0
	6	23.2	6.8	29.2
	7	18.3	7.1	38.8
	8	15.2	6.6	43.3
	9	27.5	8.1	29.5
	10	6.6	2.4	36.2
	11	6.7	2.7	39.8
	12	10.1	3.3	32.6
	13	20.5	4.8	23.4
	14	25.5	5.2	20.2
	15	13.2	6.2	46.7
	16	11.6	4.9	42.7
	17	15.8	6.4	40.3
	18	22.3	5.8	26.0
	19	15.8	5.3	33.7

TABLE 2 (continued)

WIND AZIMUTH (degrees)	MEASUREMENT LOCATION	$U/U_{\infty}$ (percent)	$U_{rms}/U_{\infty}$ (percent)	$U_{rms}/U$ (percent)
300	1	21.6	9.0	41.7
	2	9.6	4.6	48.1
	3	11.8	5.2	44.3
	4	11.4	5.0	43.7
	5	17.5	6.1	34.7
	6	22.0	8.6	39.0
	7	16.2	6.8	41.7
	8	10.7	5.4	50.3
	9	30.1	8.2	27.2
	10	6.5	2.3	35.7
	11	8.0	3.3	40.9
	12	14.4	4.7	32.4
	13	21.4	5.2	24.3
	14	20.7	4.7	22.9
	15	7.1	2.3	32.5
	16	11.0	4.8	43.8
	17	12.9	5.1	39.6
	18	21.1	4.8	22.6
	19	14.8	4.6	31.4
315	1	11.2	5.1	46.0
	2	11.1	4.9	43.8
	3	14.8	5.7	38.9
	4	22.4	7.7	34.5
	5	22.2	8.3	37.2
	6	26.2	7.9	30.0
	7	23.9	8.8	36.7
	8	25.9	7.8	30.0
	9	14.9	6.3	42.1
	10	8.9	3.6	40.5
	11	10.7	4.8	45.2
	12	12.3	5.0	40.6
	13	20.2	5.0	24.6
	14	18.4	4.8	26.0
	15	7.8	3.5	44.3
	16	12.6	5.1	40.8
	17	13.5	6.2	46.2
	18	23.7	5.3	22.3
	19	13.6	5.8	42.4

TABLE 2 (continued)

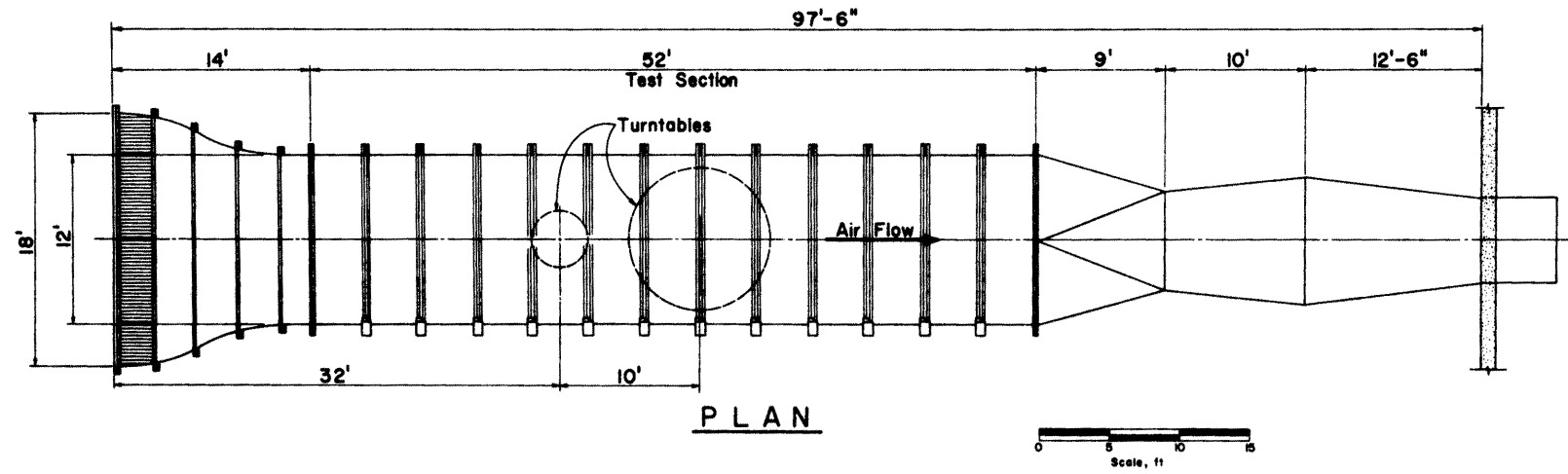
WIND AZIMUTH (degrees)	MEASUREMENT LOCATION	$U/U_{\infty}$ (percent)	$U_{rms}/U_{\infty}$ (percent)	$U_{rms}/U$ (percent)
330	1	10.2	5.0	48.8
	2	8.8	3.9	44.6
	3	18.8	6.1	32.7
	4	24.1	8.4	34.7
	5	21.3	9.0	42.4
	6	21.1	8.8	41.5
	7	20.8	8.5	40.7
	8	18.1	7.6	41.9
	9	16.3	8.1	49.9
	10	11.3	4.9	43.3
	11	11.1	4.8	43.3
	12	8.4	3.7	43.7
	13	7.7	2.3	29.5
	14	4.4	1.3	28.9
	15	14.2	6.8	47.6
	16	13.5	5.7	42.4
	17	12.0	5.4	45.2
	18	15.5	4.9	31.5
	19	8.9	3.9	44.0
345	1	24.5	10.3	42.1
	2	21.2	8.0	37.9
	3	23.1	7.7	33.5
	4	27.6	11.5	41.6
	5	21.9	11.9	54.4
	6	16.8	9.4	56.2
	7	14.7	6.6	44.9
	8	14.7	7.4	50.3
	9	28.4	12.3	43.2
	10	11.0	4.7	42.8
	11	13.7	5.1	37.4
	12	4.7	1.4	29.3
	13	2.9	.6	19.7
	14	3.9	.8	21.4
	15	22.4	8.7	39.0
	16	16.1	6.1	37.6
	17	23.2	8.5	36.5
	18	13.3	5.4	40.4
	19	10.0	4.1	40.7

TABLE 3

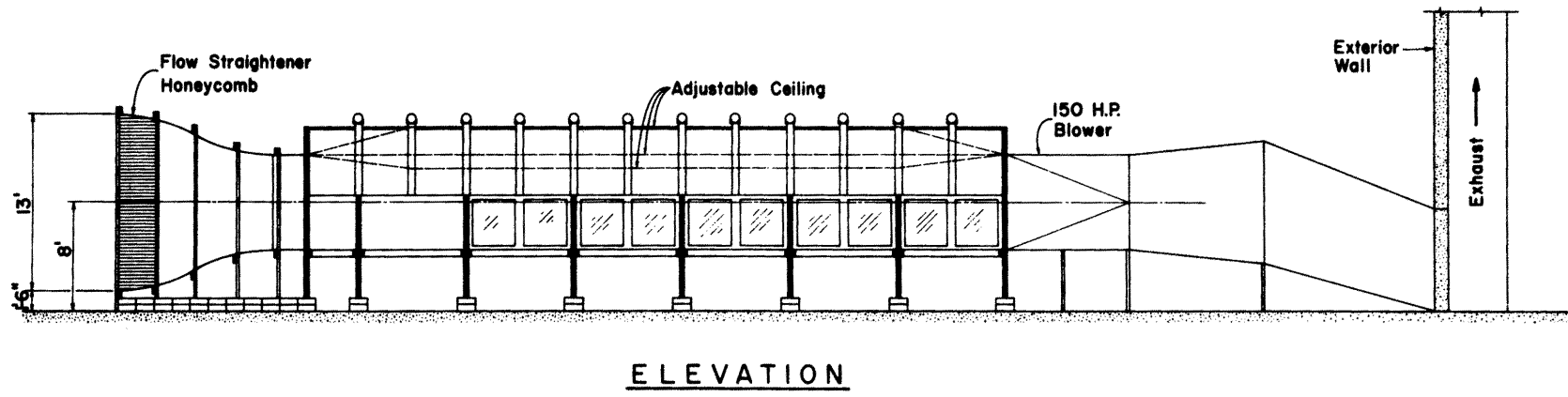
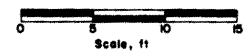
PRESSURE DATA FOR EAST AND WEST SIDES OF  
UNIVERSITY OF PENNSYLVANIA HOSPITAL ADDITION

WIND AZIMUTH	EAST TAP ( $P_1$ )	WEST TAP ( $P_2$ )	$P_1 - P_2$
	$C_{P_{mean}}$	$C_{P_{mean}}$	$\Delta C_{P_{mean}}$
000	-0.094	-0.176	0.071
015	-0.135	-0.247	0.082
030	-0.206	-0.341	0.124
045	-0.176	-0.382	0.188
060	-0.065	-0.271	0.188
075	-0.018	-0.147	0.124
090	0.106	-0.147	0.265
105	0.012	-0.147	0.171
120	0.124	-0.206	0.353
135	0.088	-0.241	0.329
150	0.000	-0.253	0.259
165	-0.141	-0.259	0.106
180	-0.324	-0.224	-0.071
195	-0.324	-0.153	-0.165
210	-0.365	-0.076	-0.276
225	-0.365	-0.029	-0.335
240	-0.335	0.000	-0.329
255	-0.229	0.000	-0.218
270	-0.159	0.047	-0.218
285	-0.118	0.053	-0.188
300	-0.100	0.000	-0.088
315	-0.100	-0.012	-0.088
330	-0.106	-0.082	-0.006
345	-0.118	-0.153	0.024

BAROMETRIC PRESSURE 24.68 in Hg  
 TEMPERATURE 65.0 degrees F  
 VELOCITY 22.11 ft/sec



P L A N



E L E V A T I O N

Figure 1. Environmental Wind Tunnel.

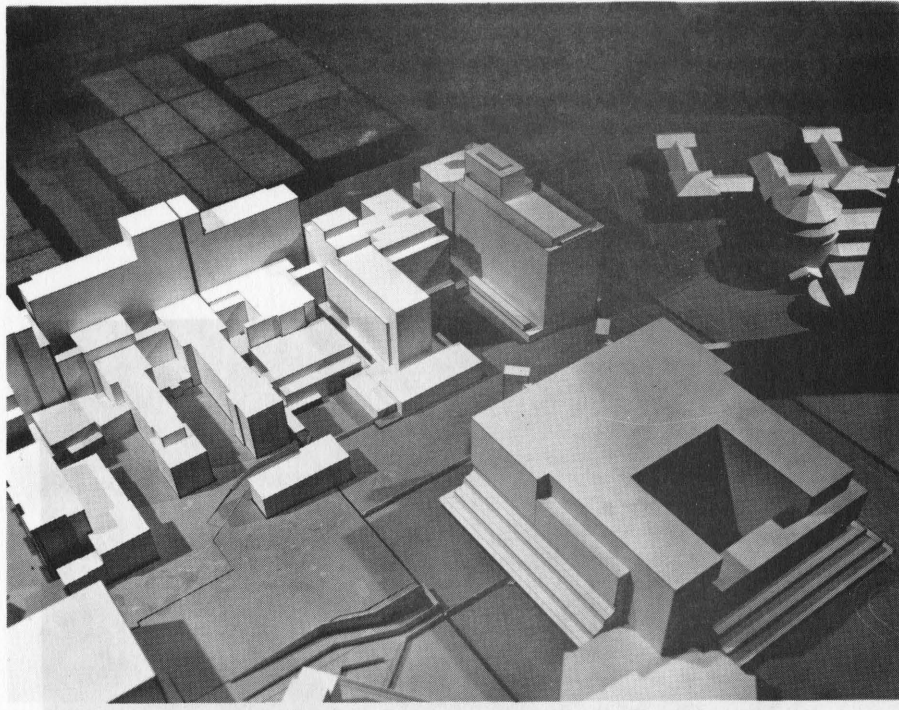


Figure 2a. Model Configuration A.

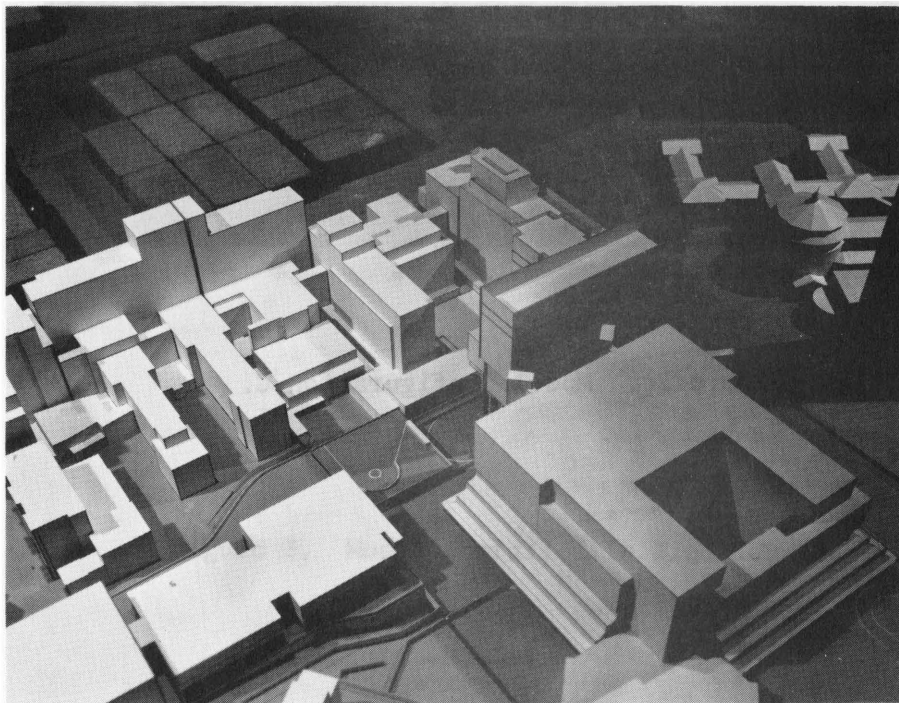


Figure 2b. Model Configuration B.

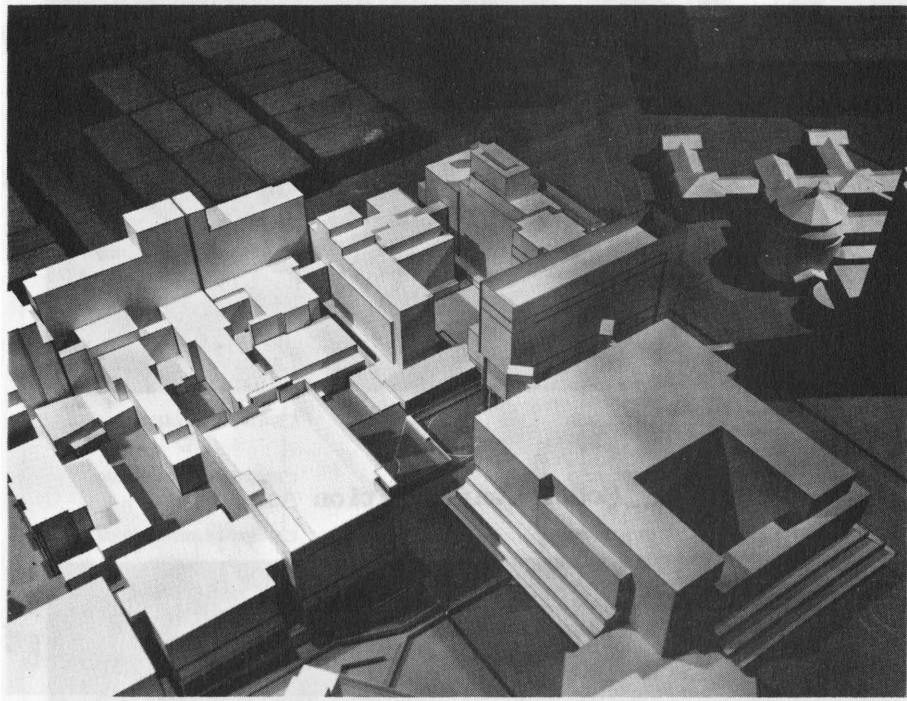


Figure 2c. Model Configuration C.



Figure 3. Model Installed in Wind Tunnel.

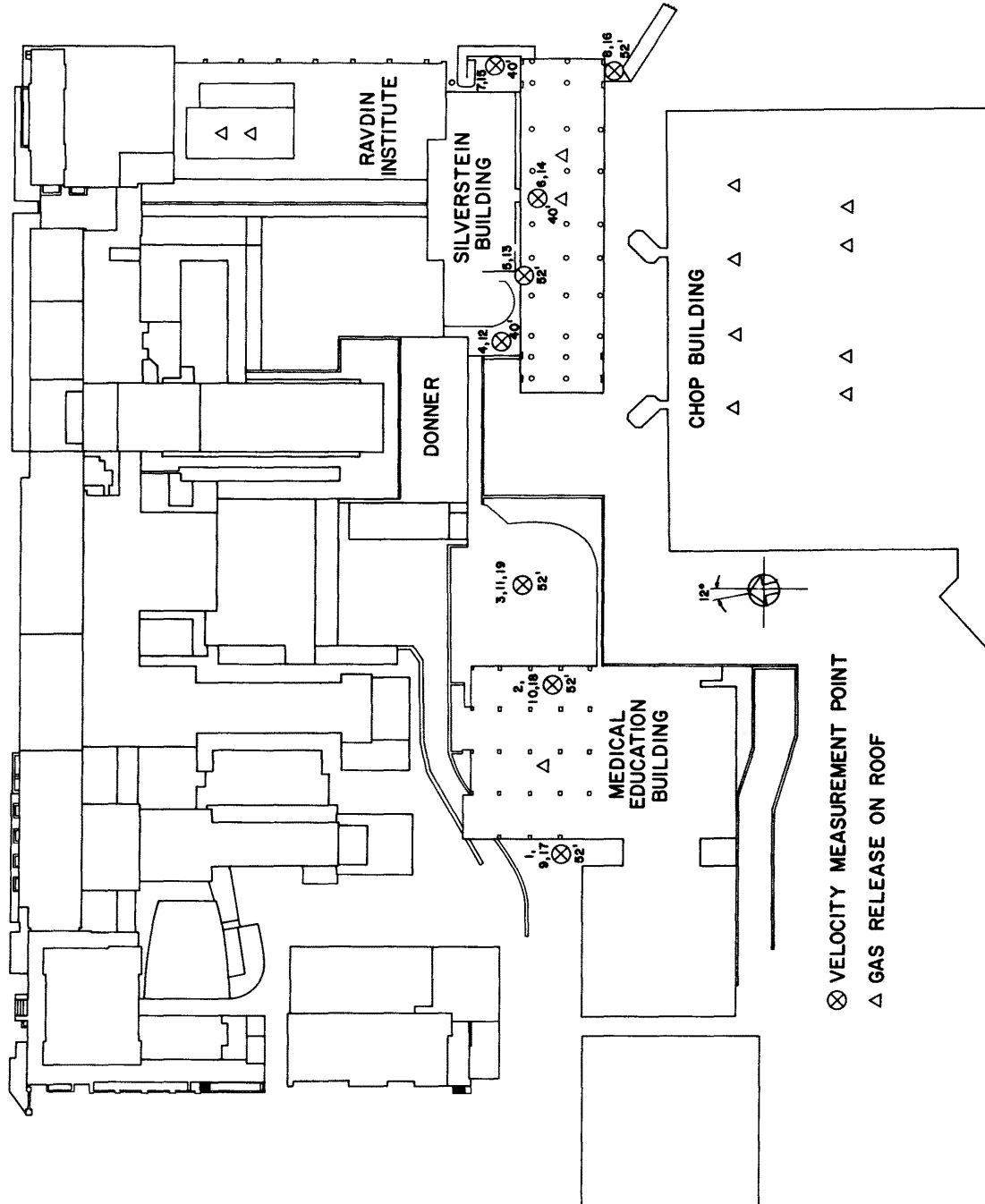


Figure 4. Velocity Measurement and Gas Discharge Locations.

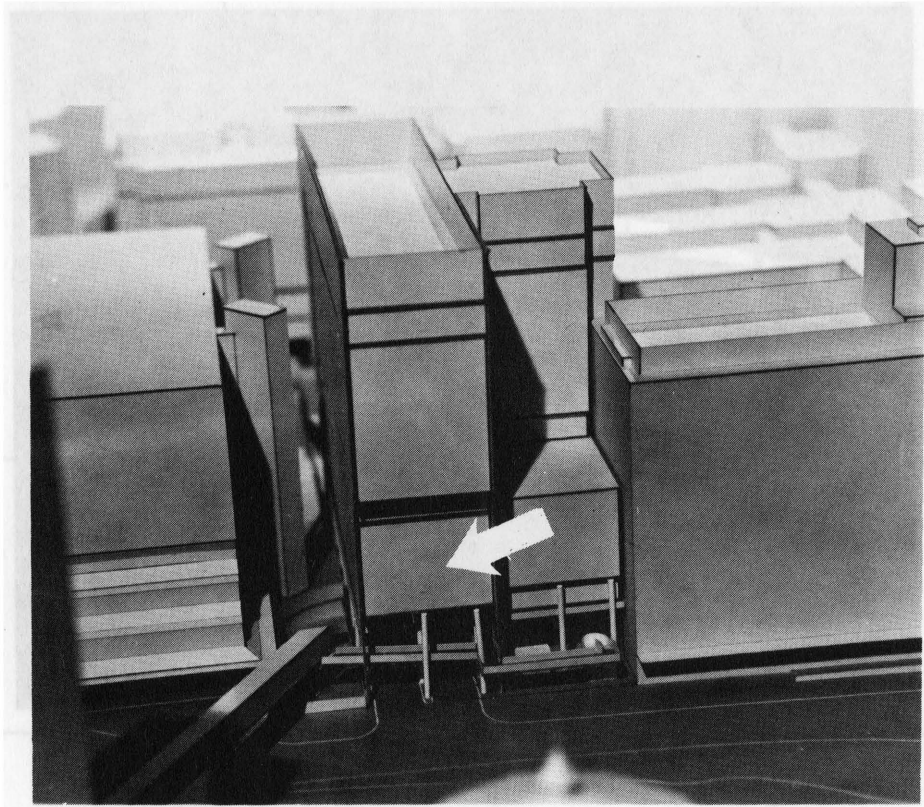


Figure 5. Pressure Tap Locations.

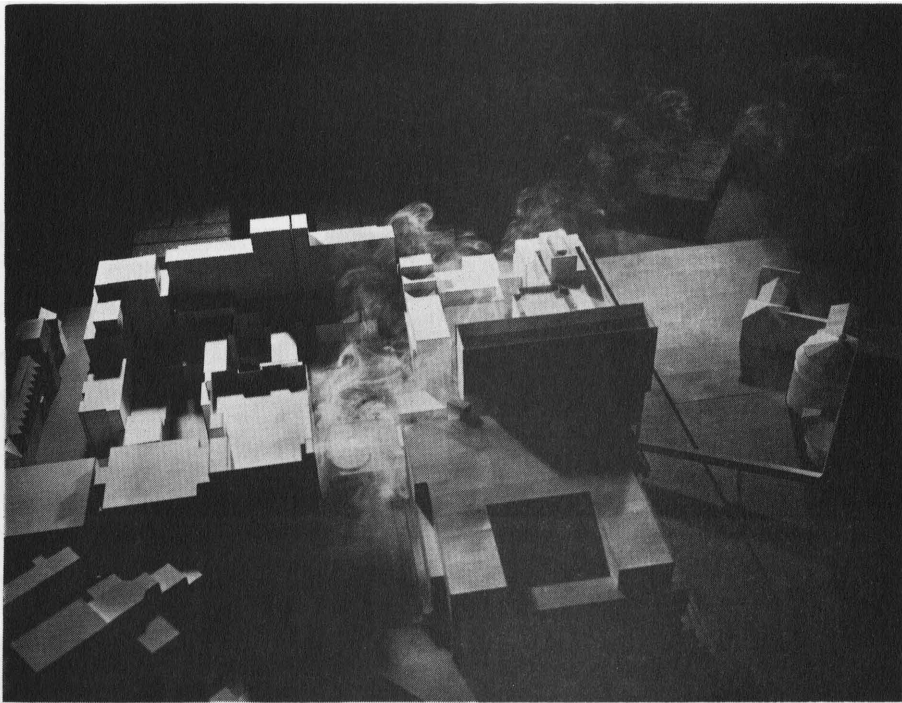


Figure 6. Flow Visualization Using Smoke.

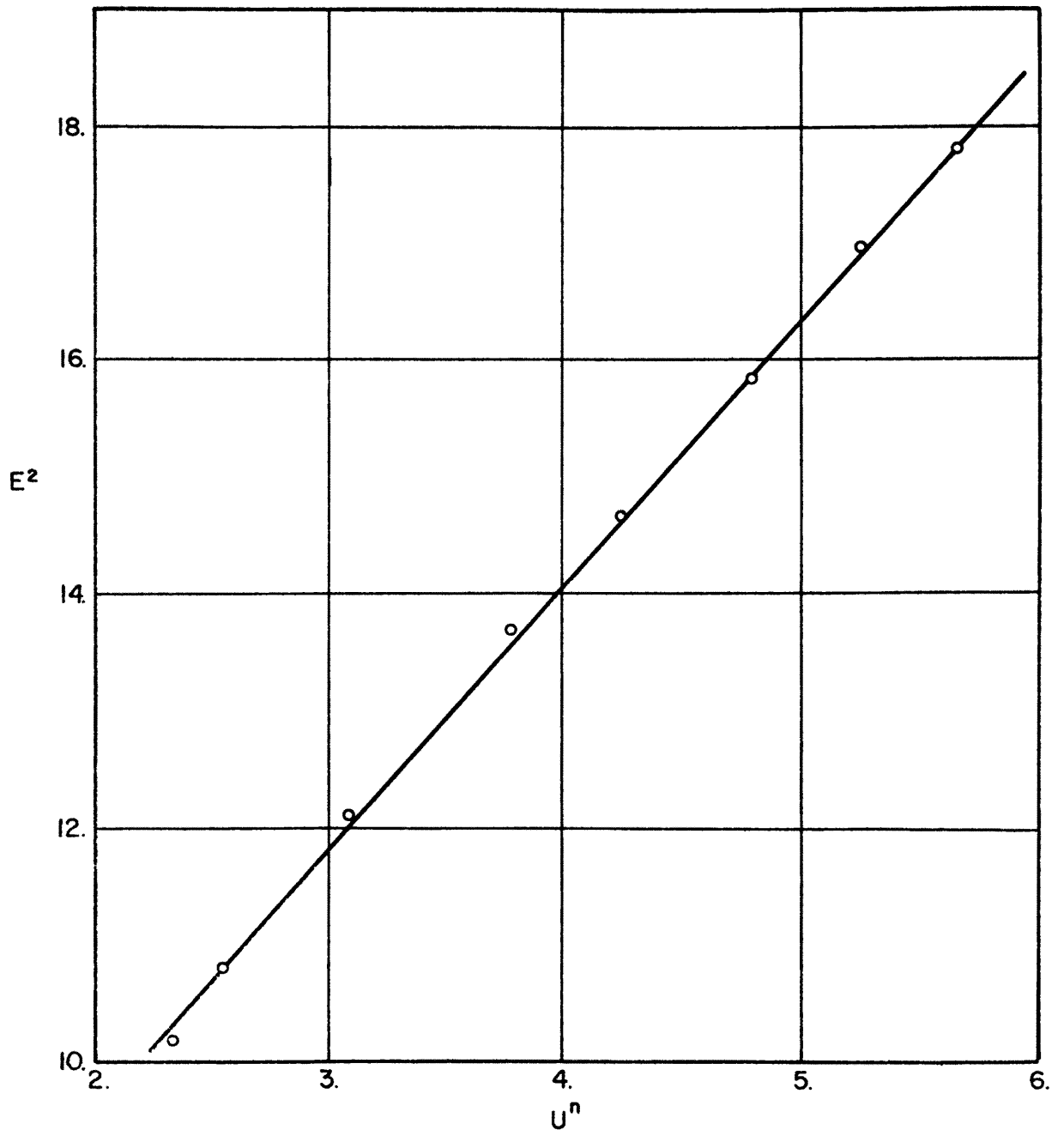


Figure 7. Typical Hot-Wire Calibration.

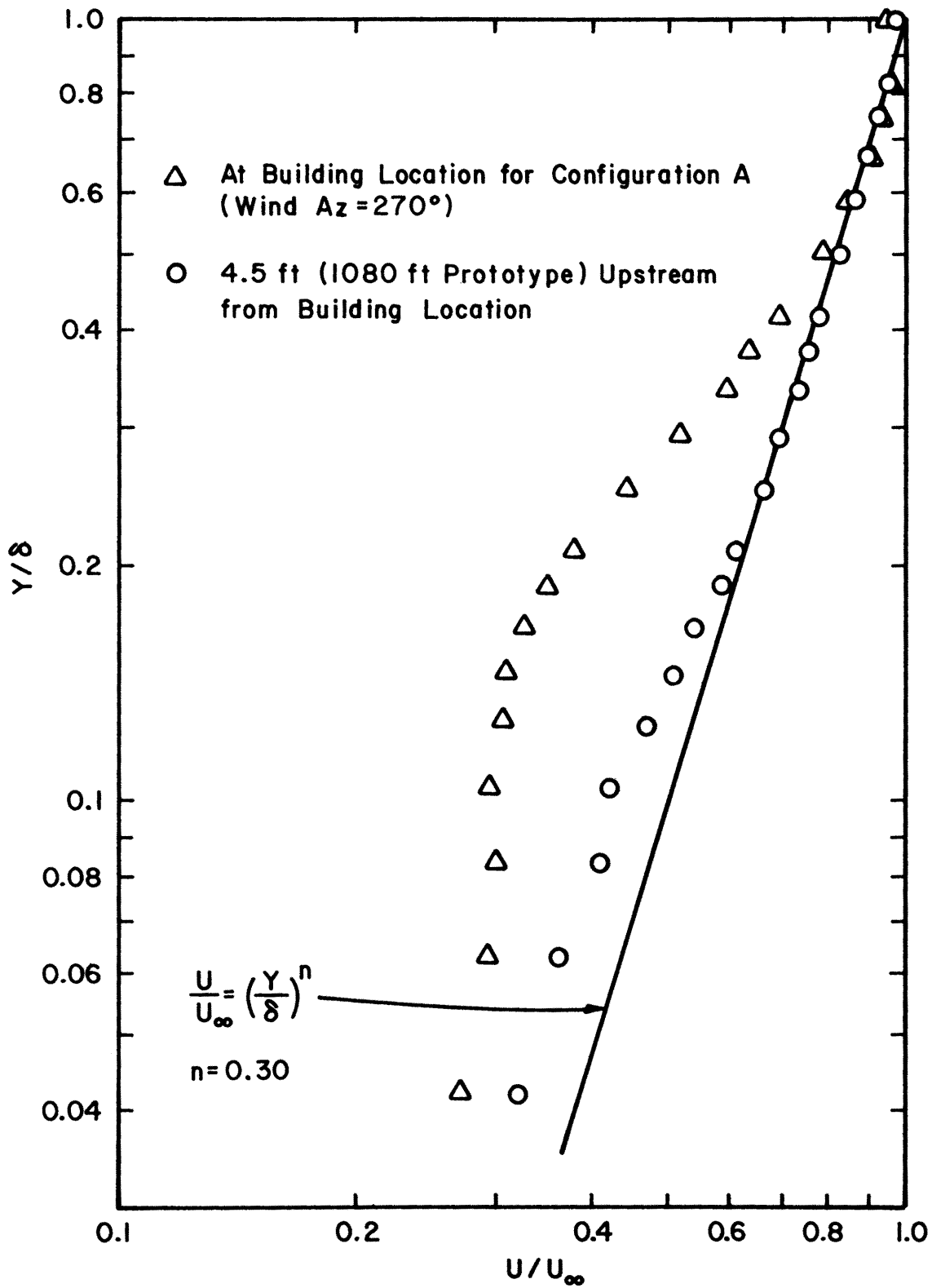


Figure 8a. Mean Velocity Profiles Approaching the Model.

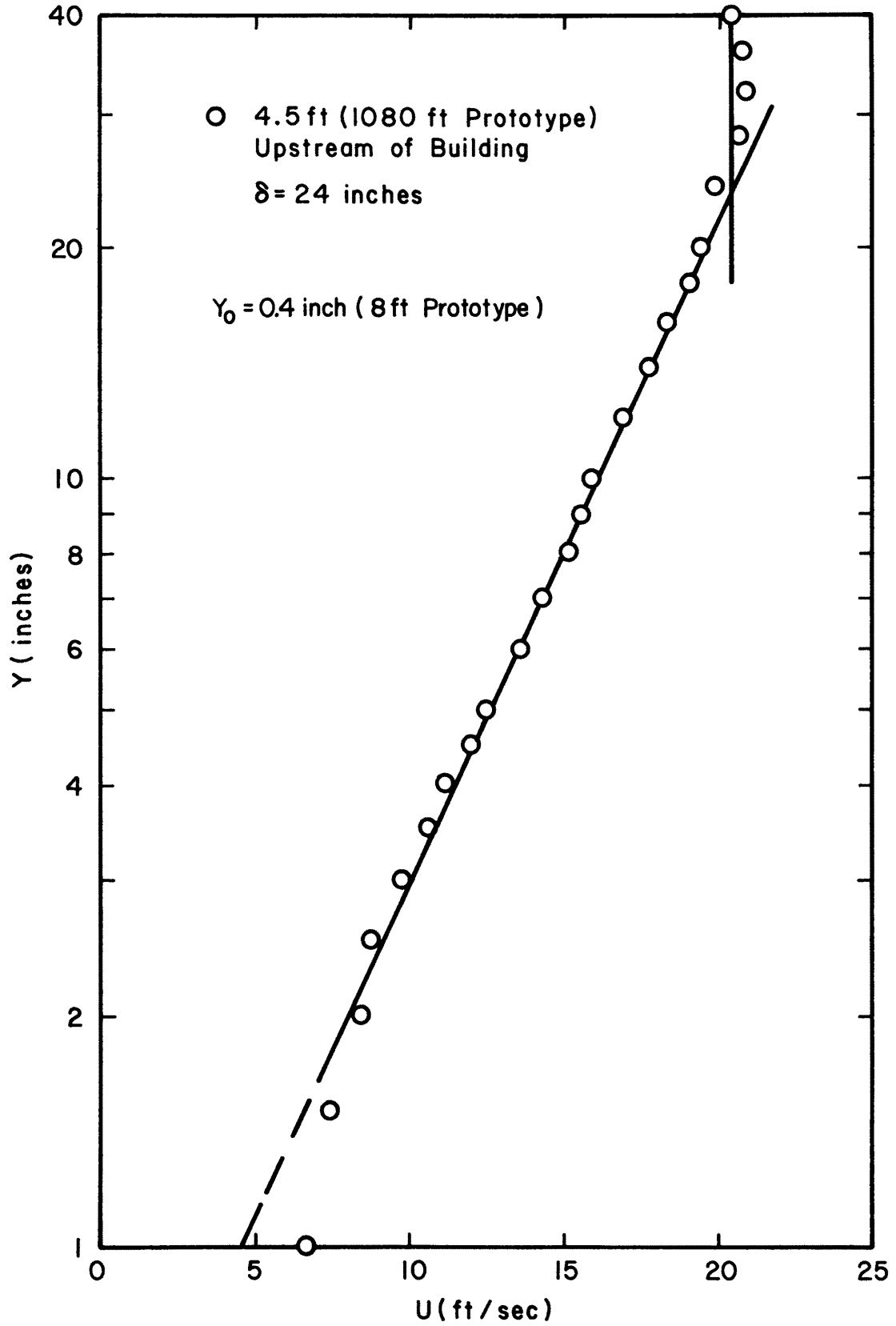


Figure 8b. Mean Velocity Profiles Approaching the Model.

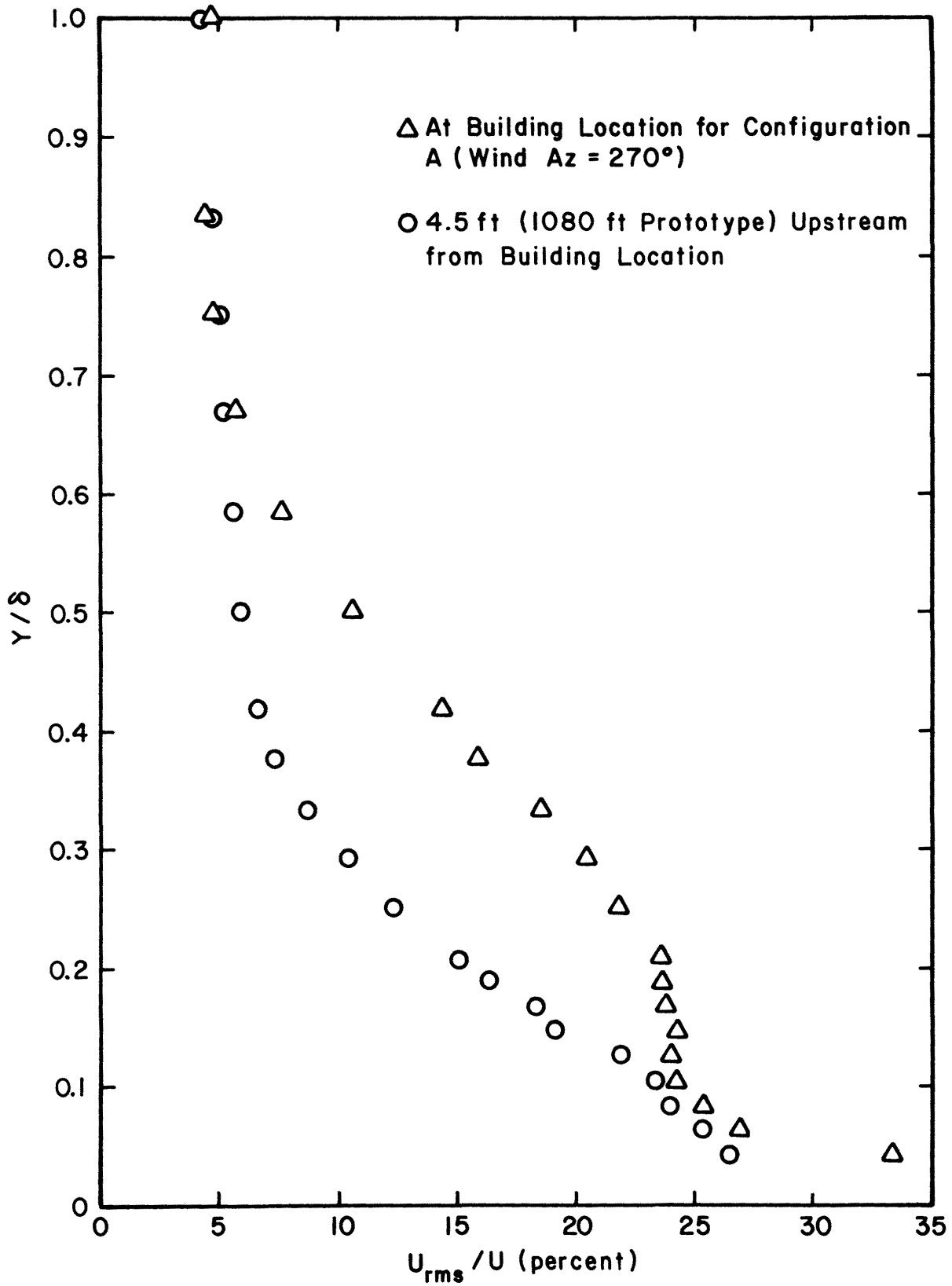


Figure 9. Turbulence Intensity Profiles.

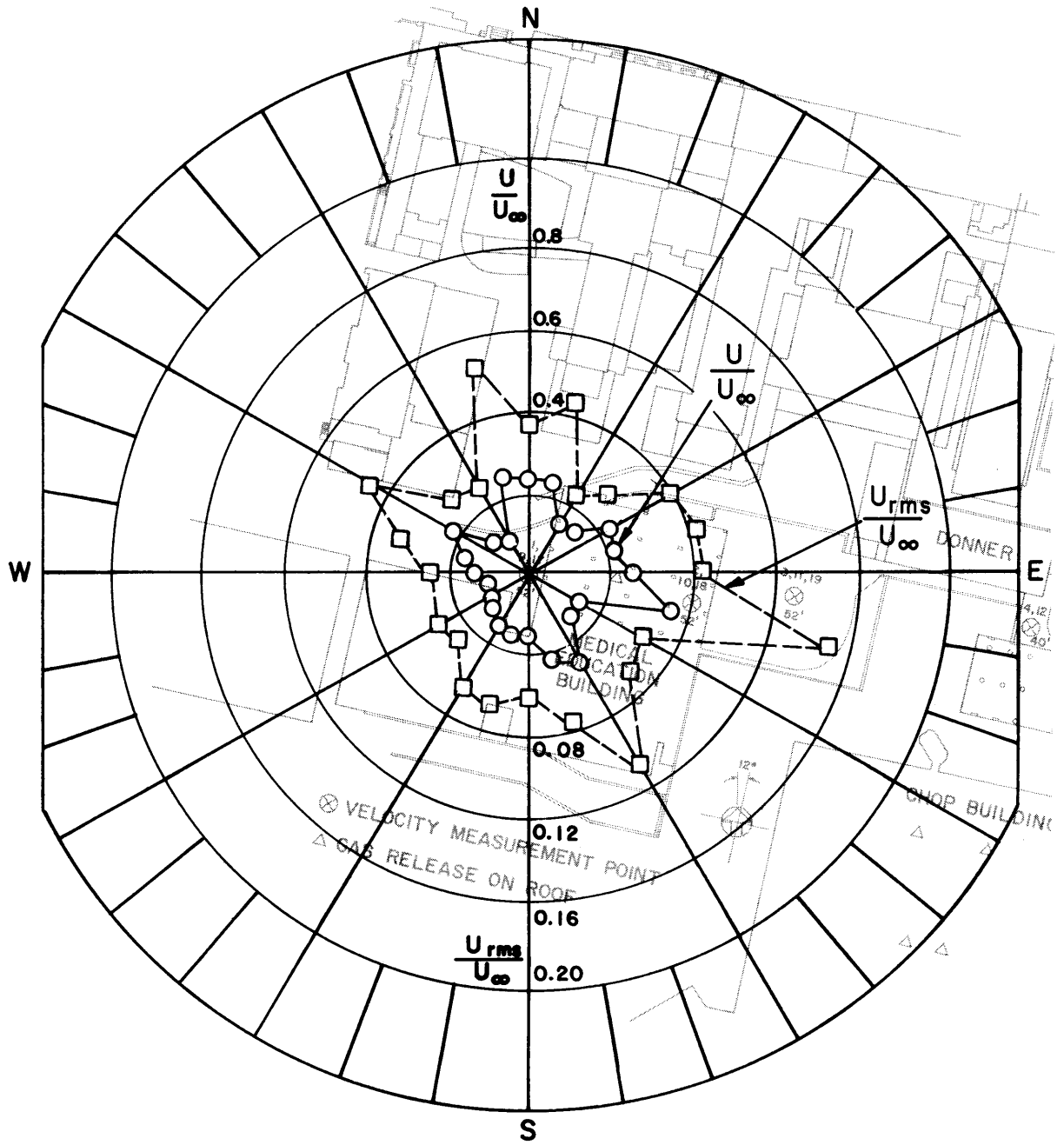


Figure 10. Mean Velocity and Turbulence Intensity at Point 1.

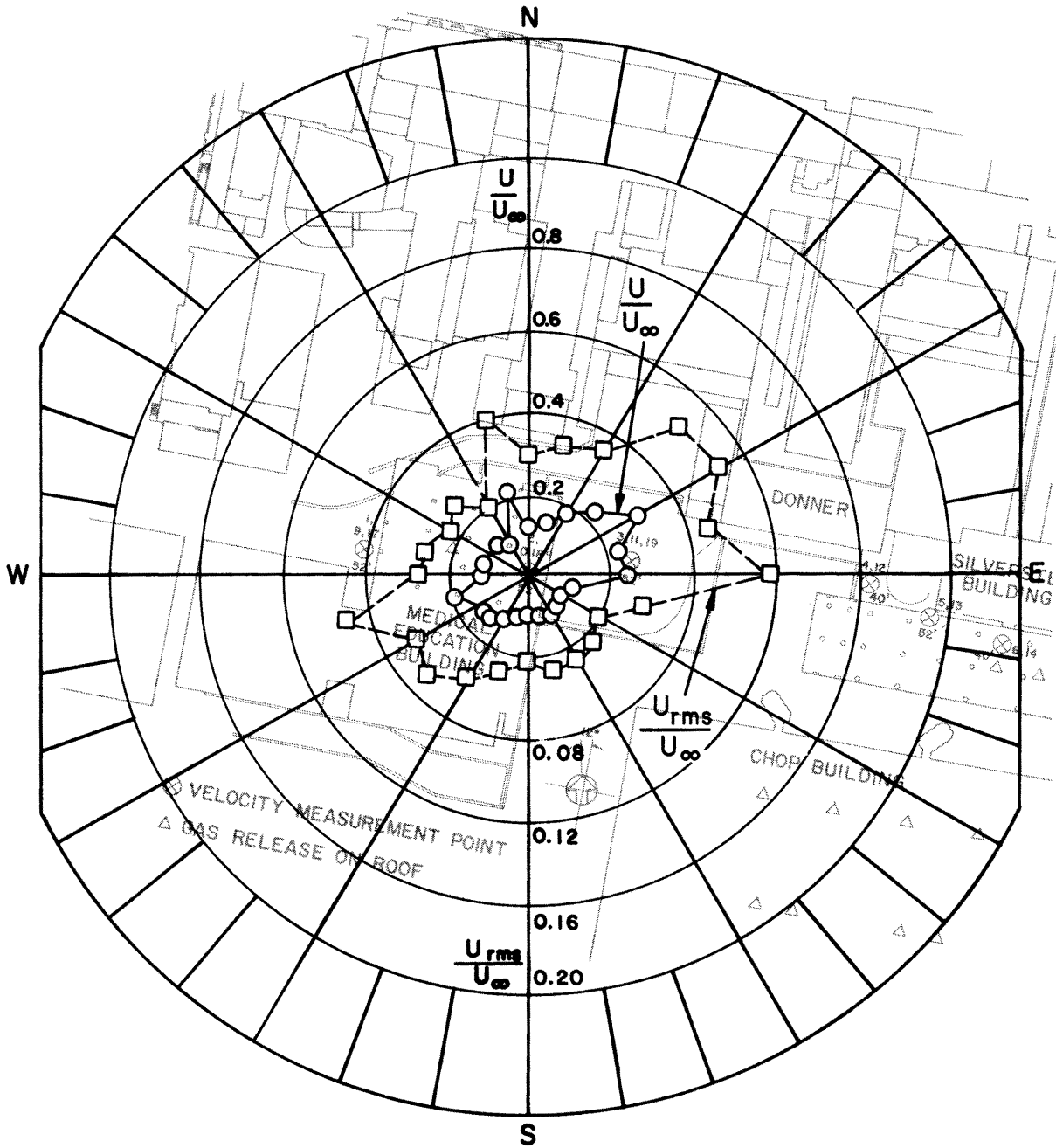


Figure 11. Mean Velocity and Turbulence Intensity at Point 2.

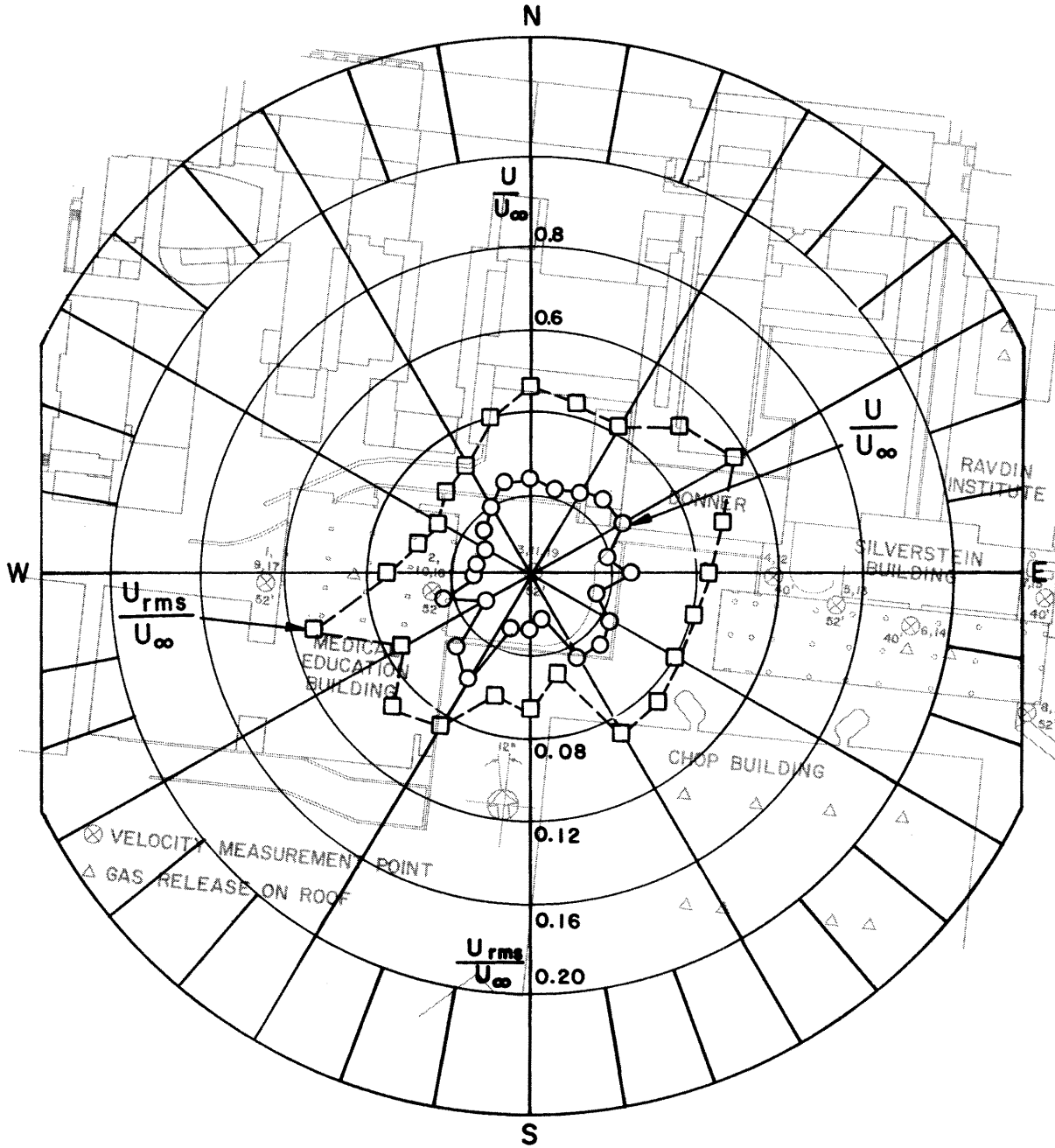


Figure 12. Mean Velocity and Turbulence Intensity at Point 3.

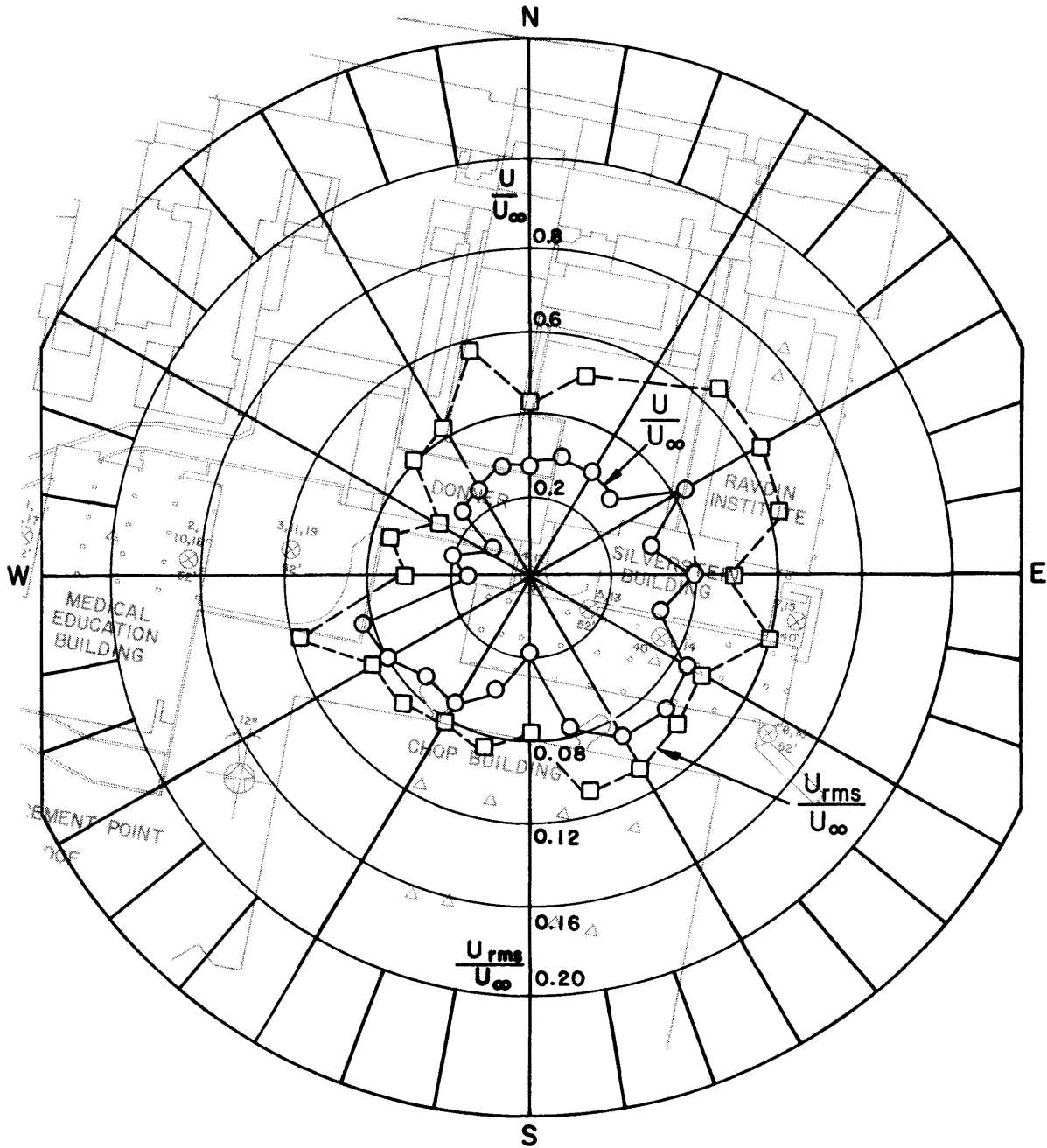


Figure 13. Mean Velocity and Turbulence Intensity at Point 4.

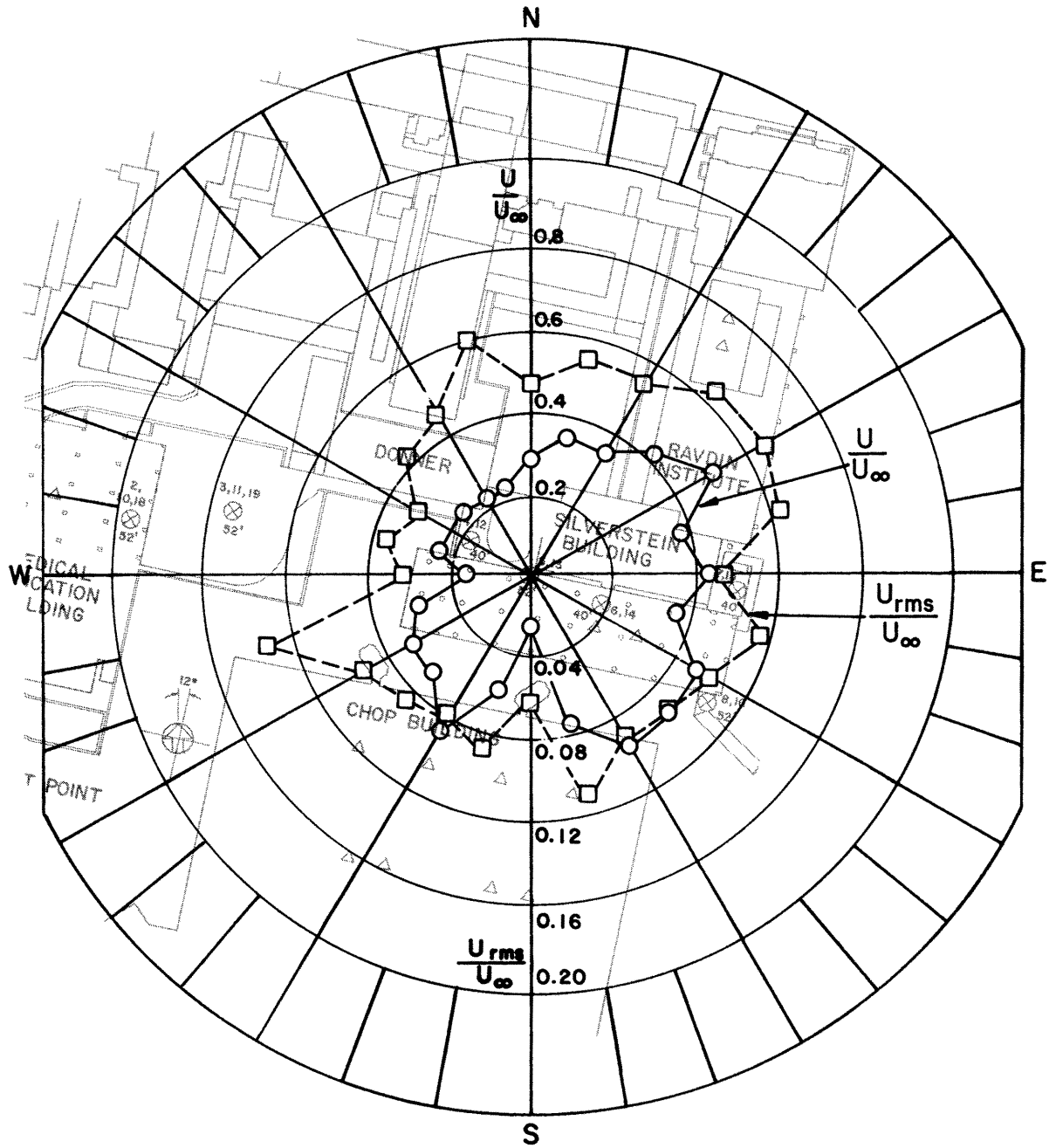


Figure 14. Mean Velocity and Turbulence Intensity at Point 5.

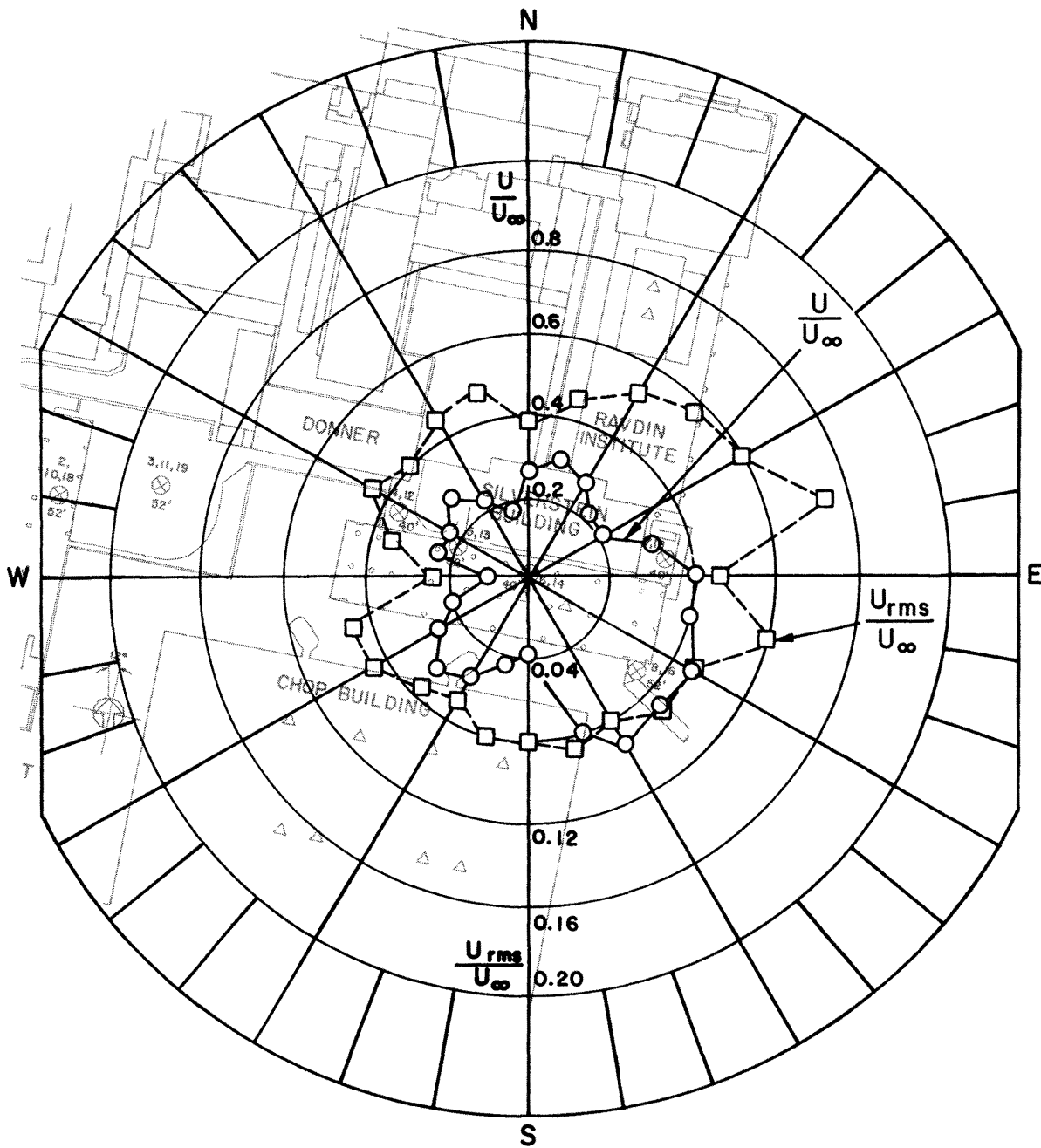


Figure 15. Mean Velocity and Turbulence Intensity at Point 6.

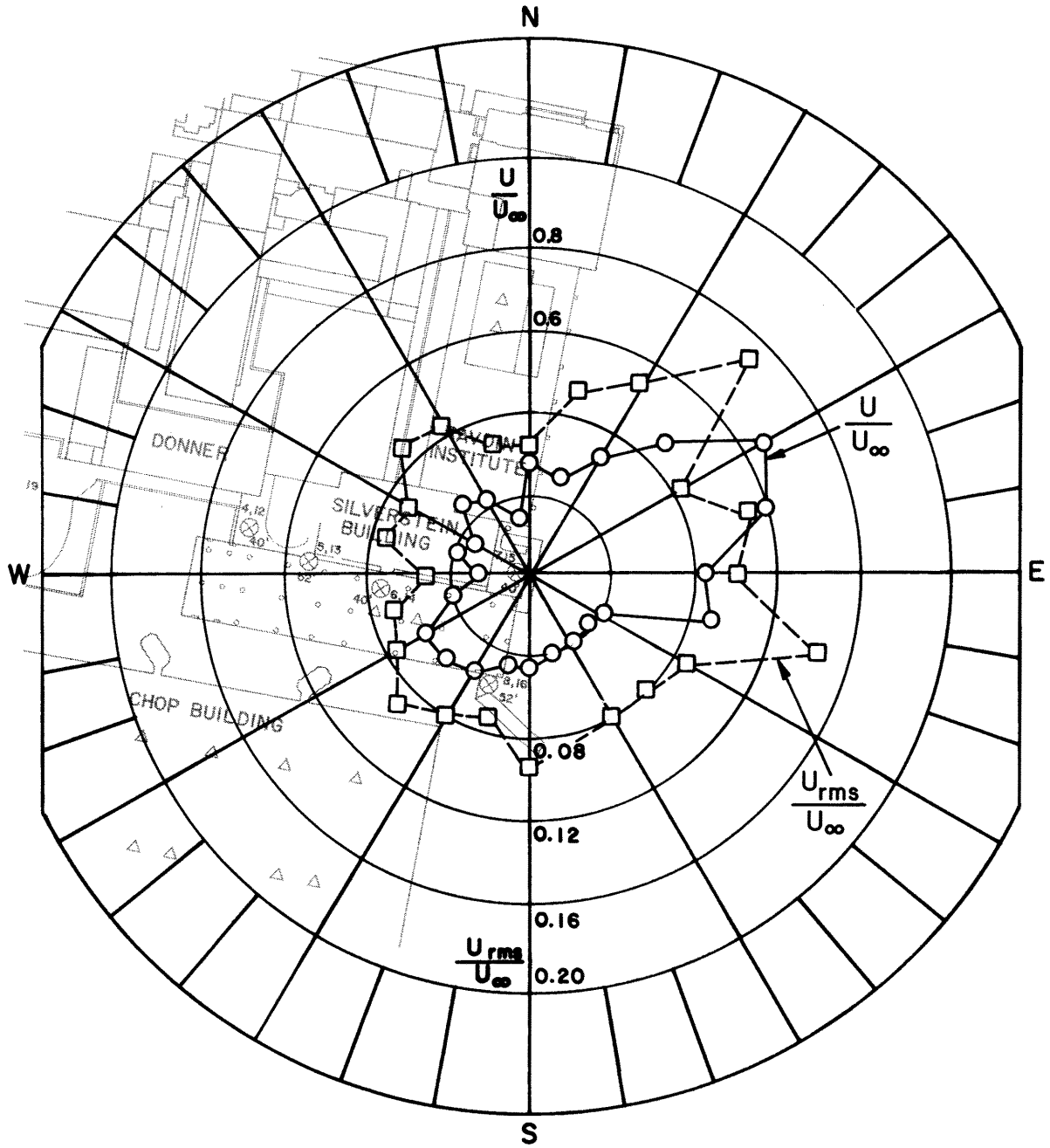


Figure 16. Mean Velocity and Turbulence Intensity at Point 7.

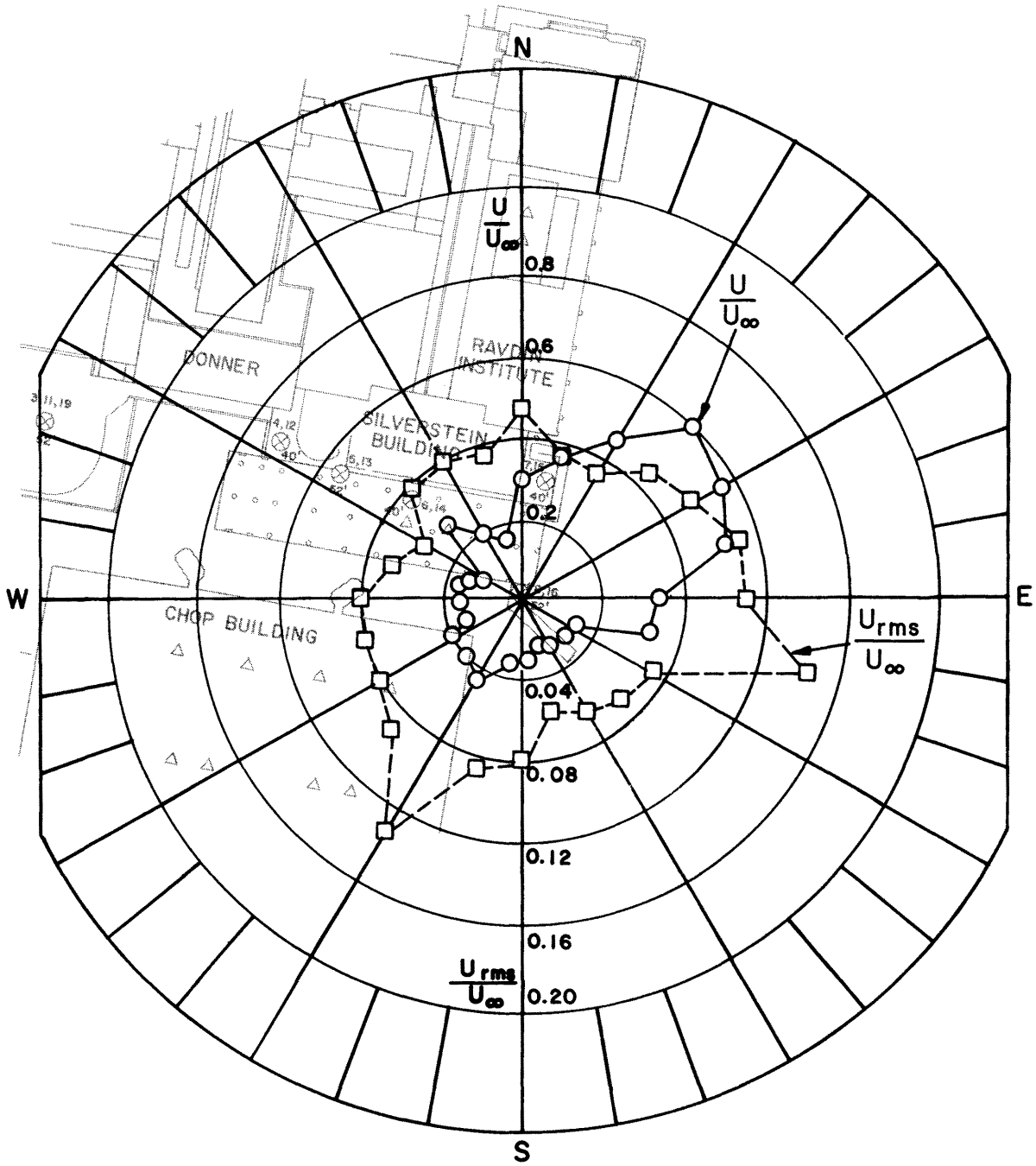


Figure 17. Mean Velocity and Turbulence Intensity at Point 8.

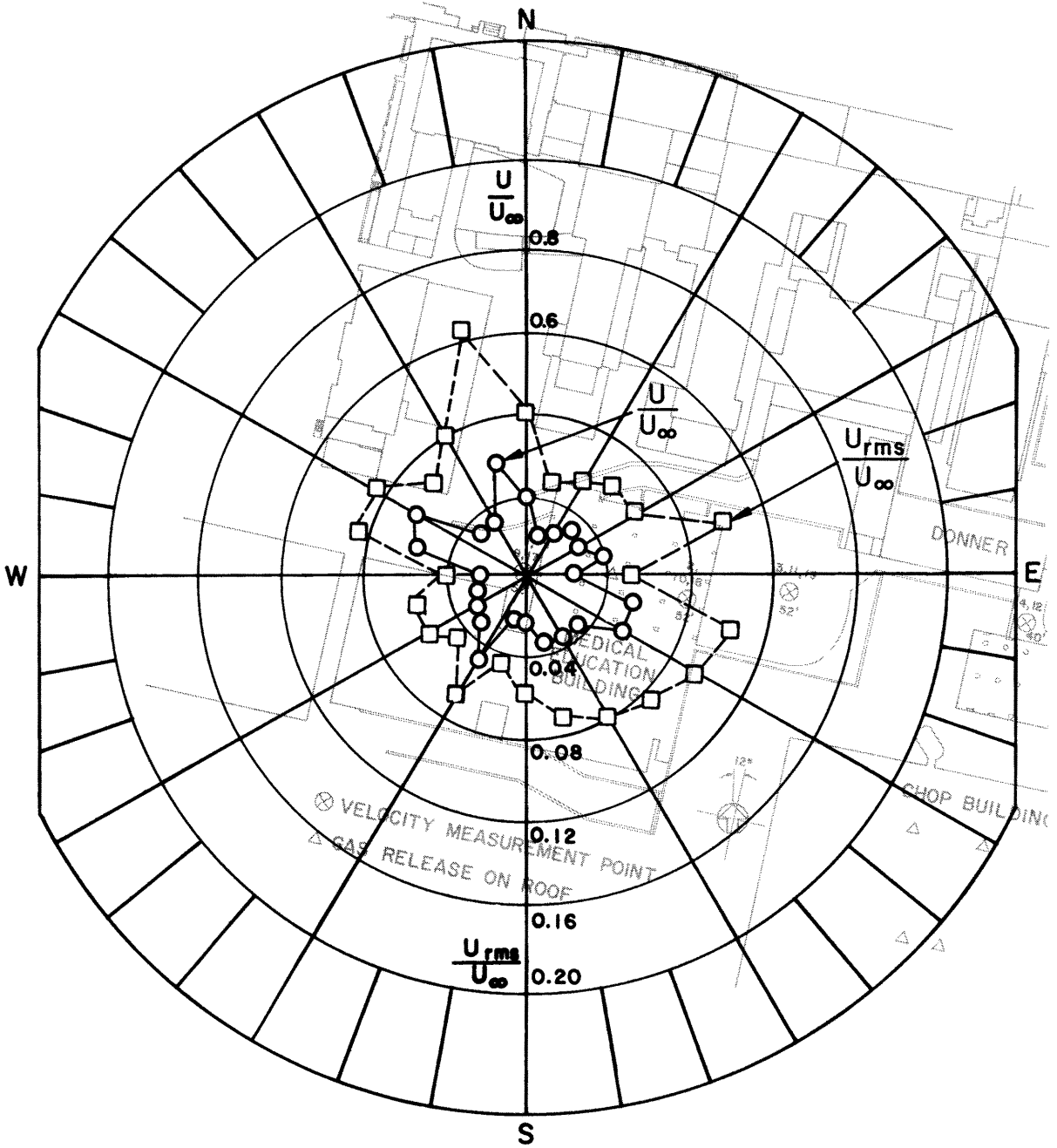


Figure 18. Mean Velocity and Turbulence Intensity at Point 9.

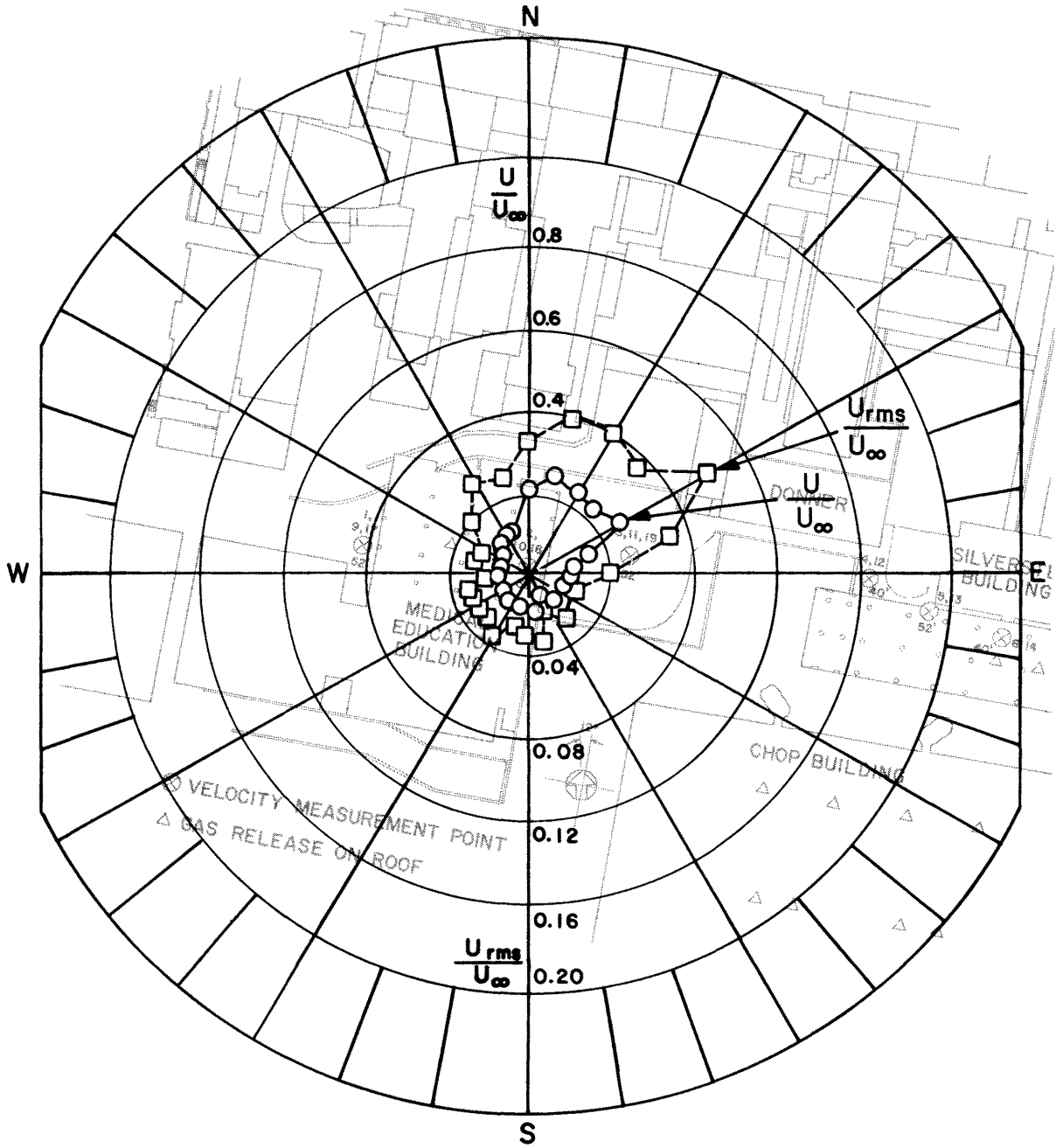


Figure 19. Mean Velocity and Turbulence Intensity at Point 10.

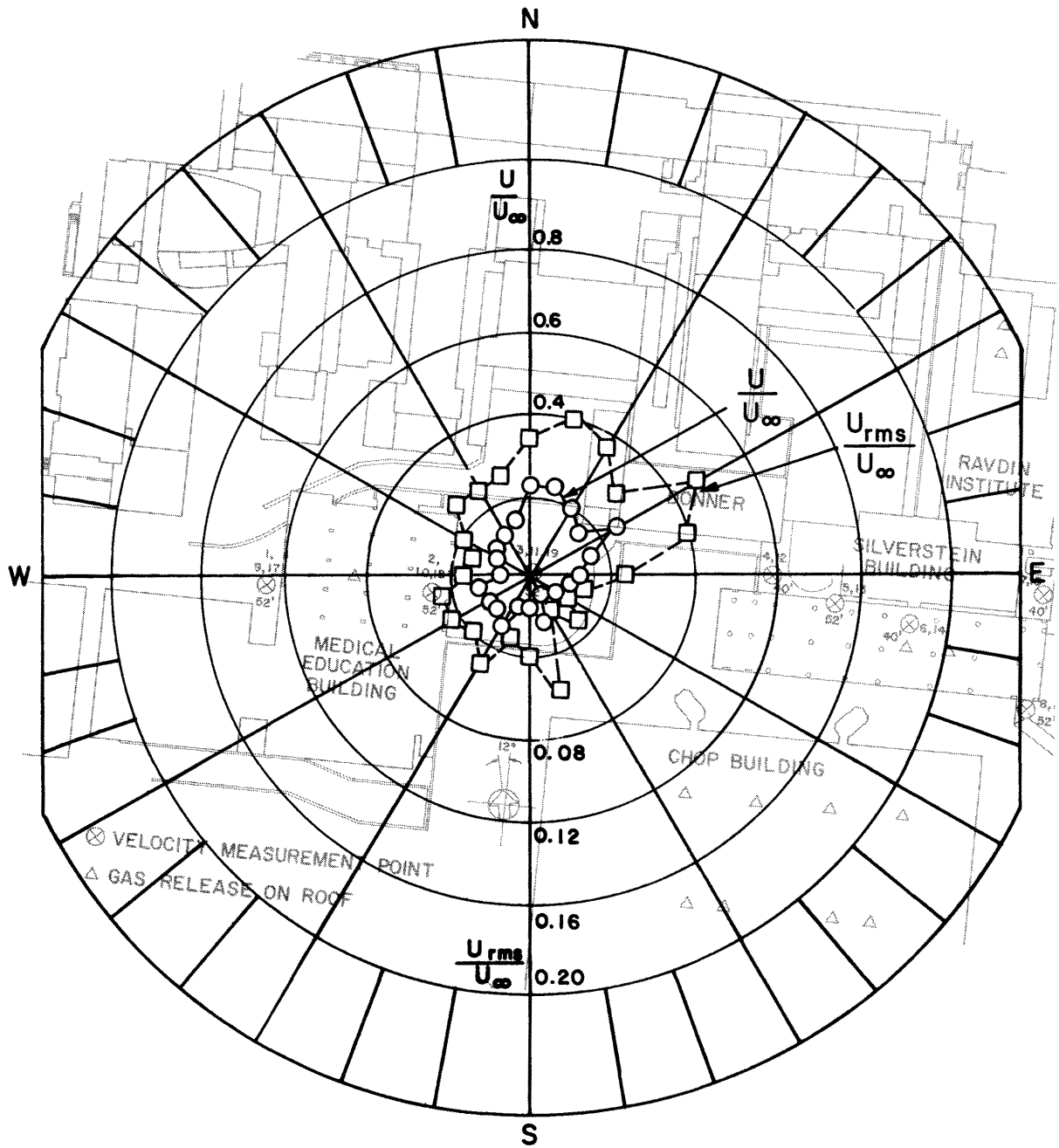


Figure 20. Mean Velocity and Turbulence Intensity at Point 11.

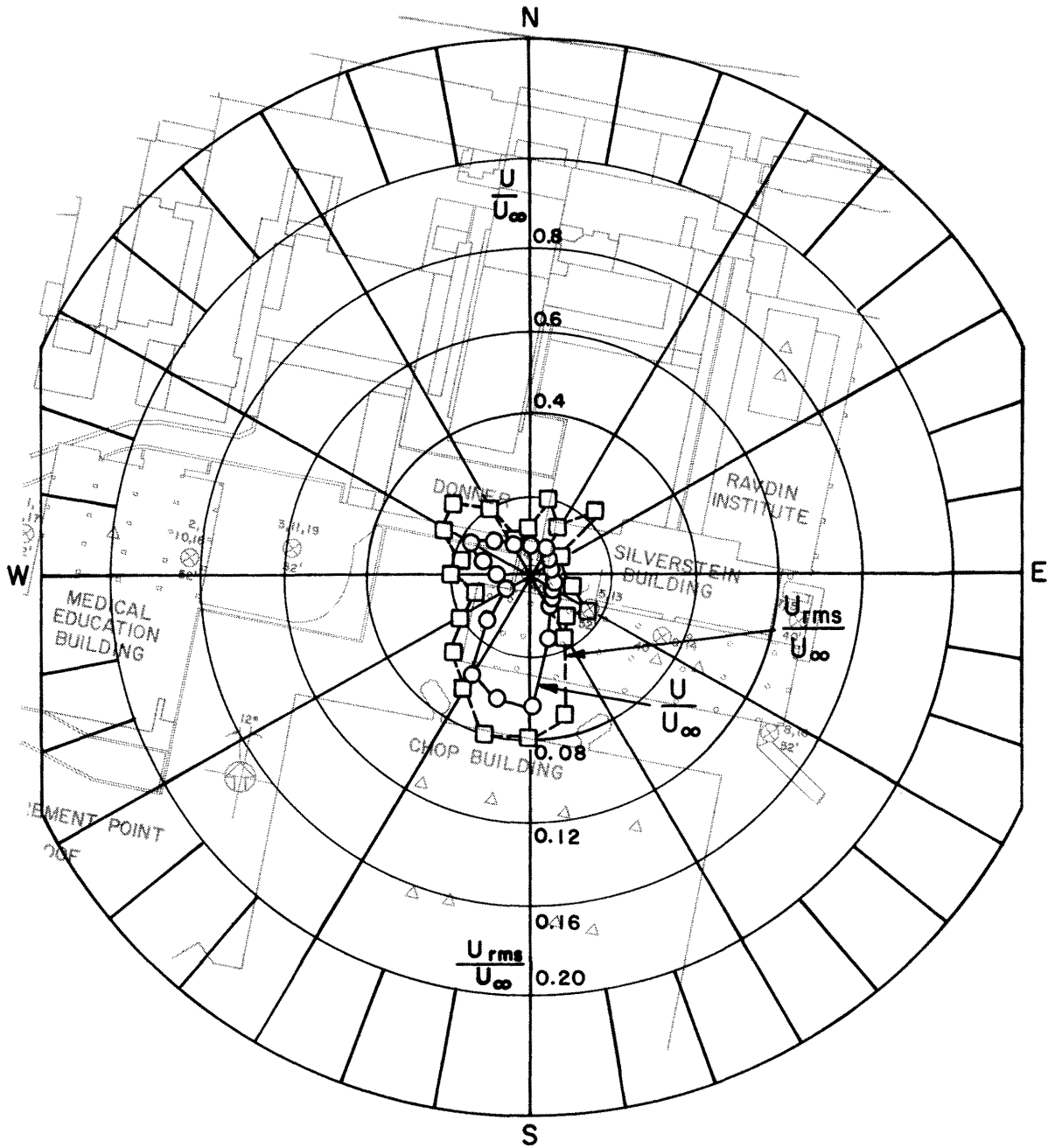


Figure 21. Mean Velocity and Turbulence Intensity at Point 12.

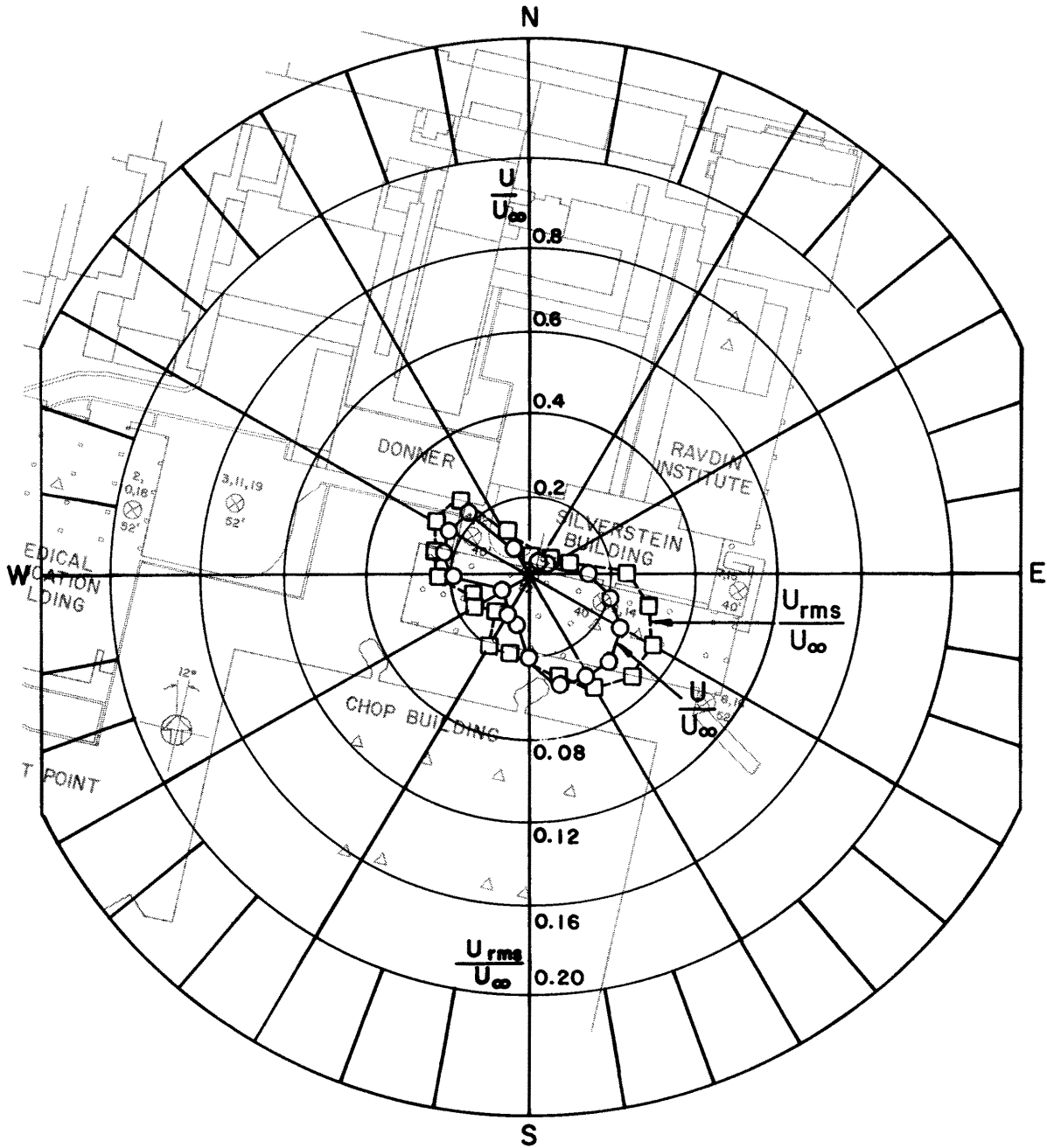


Figure 22. Mean Velocity and Turbulence Intensity at Point 13.

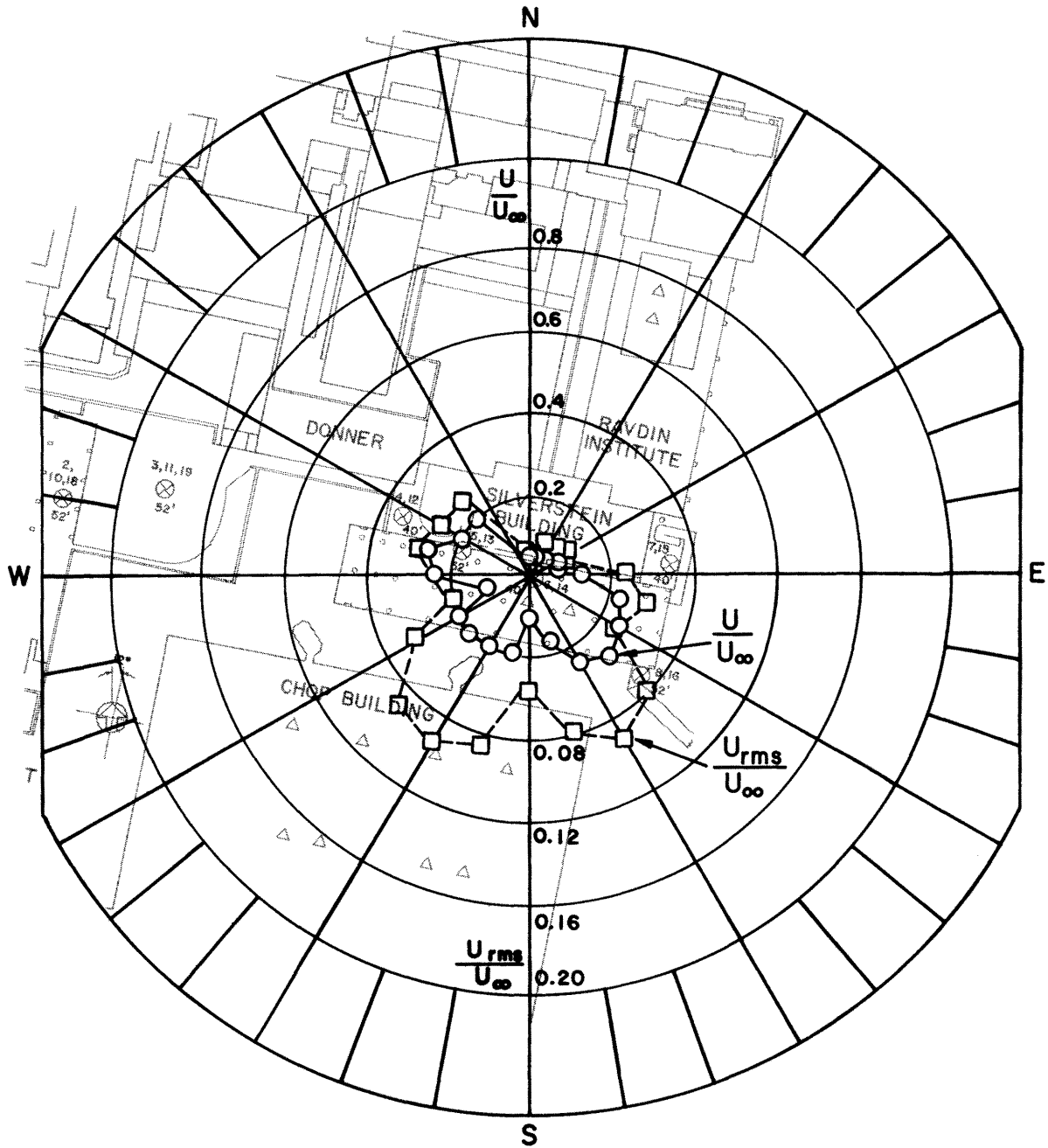


Figure 23. Mean Velocity and Turbulence Intensity at Point 14.

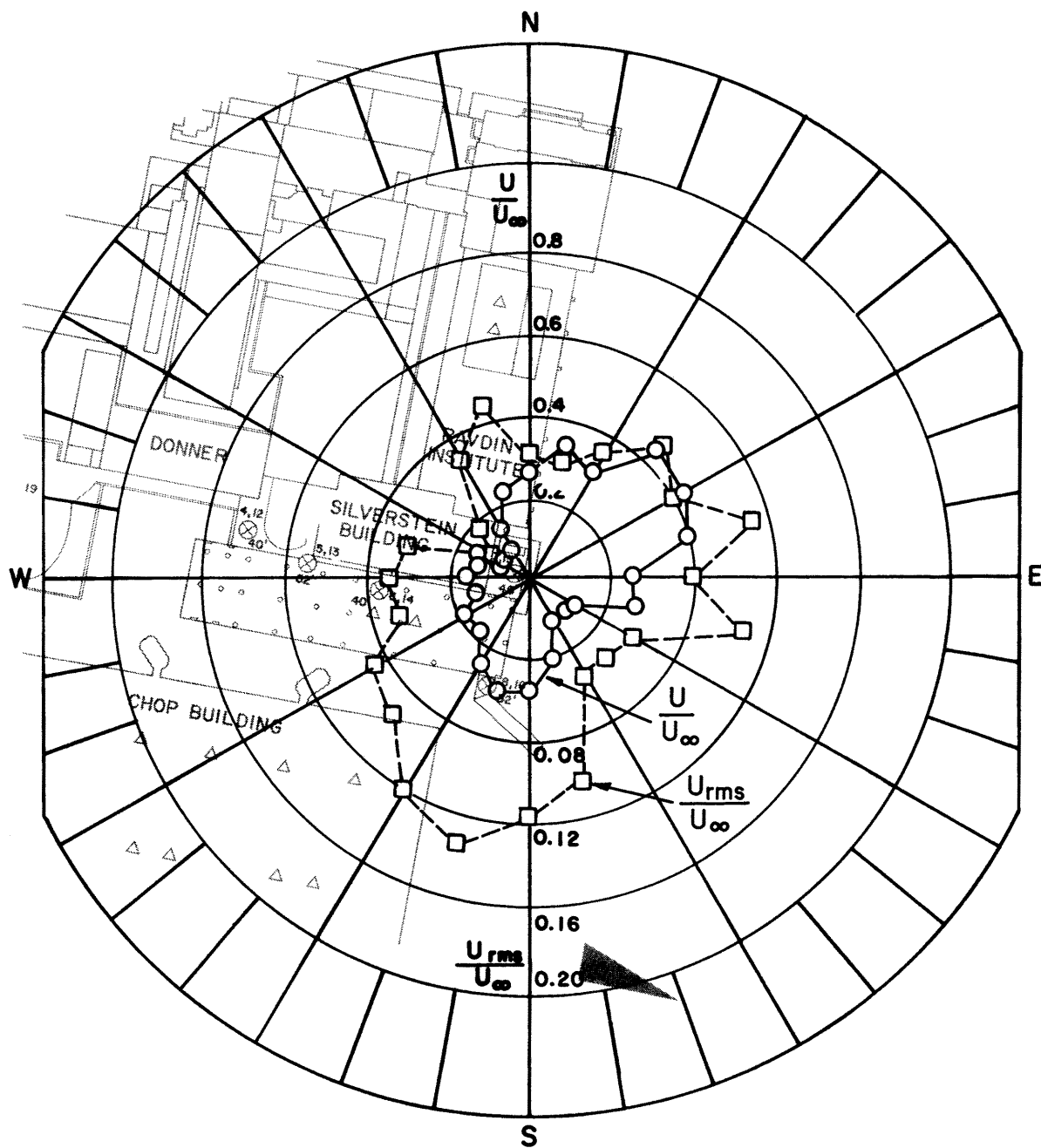


Figure 24. Mean Velocity and Turbulence Intensity at Point 15.

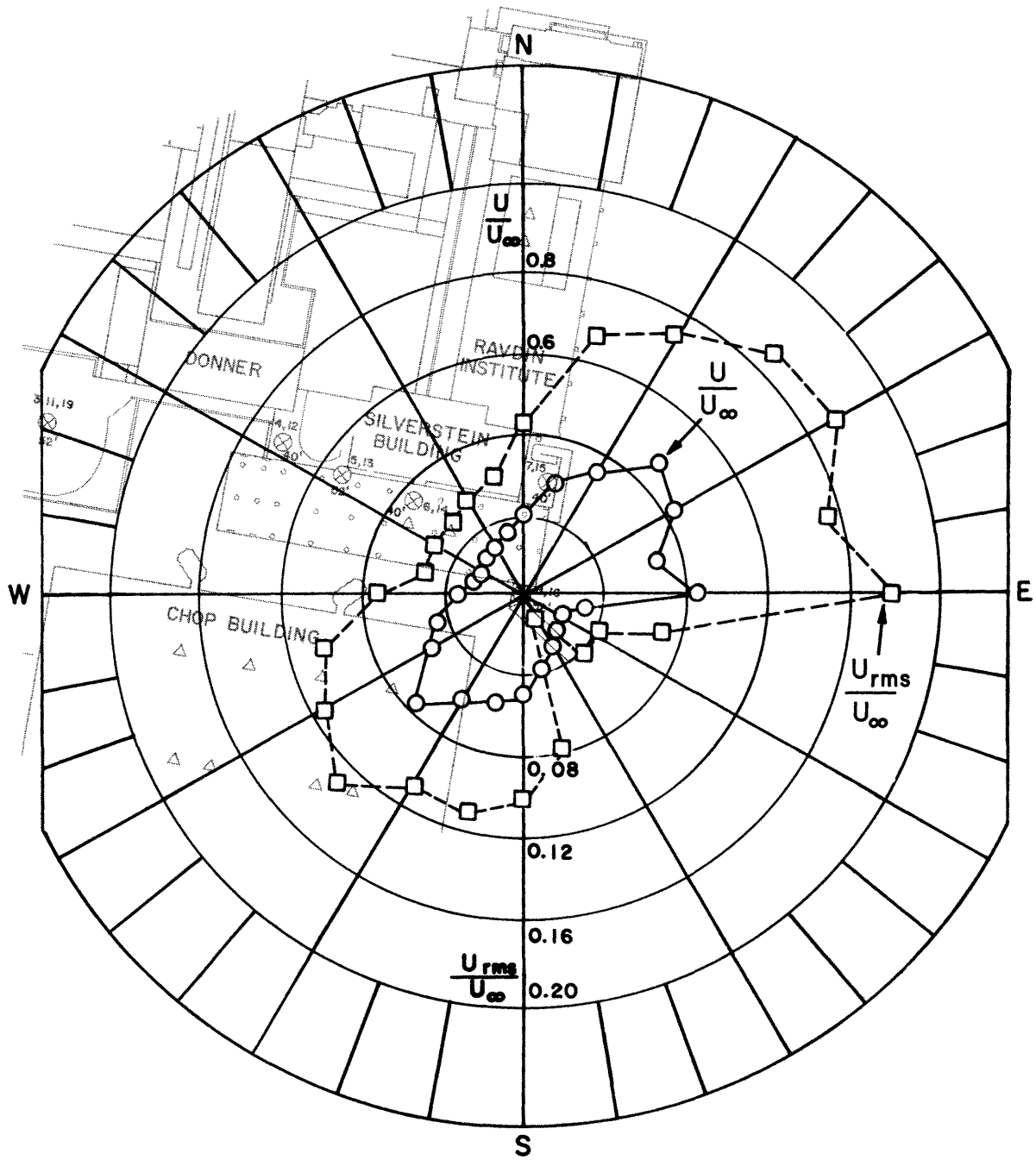


Figure 25. Mean Velocity and Turbulence Intensity at Point 16.

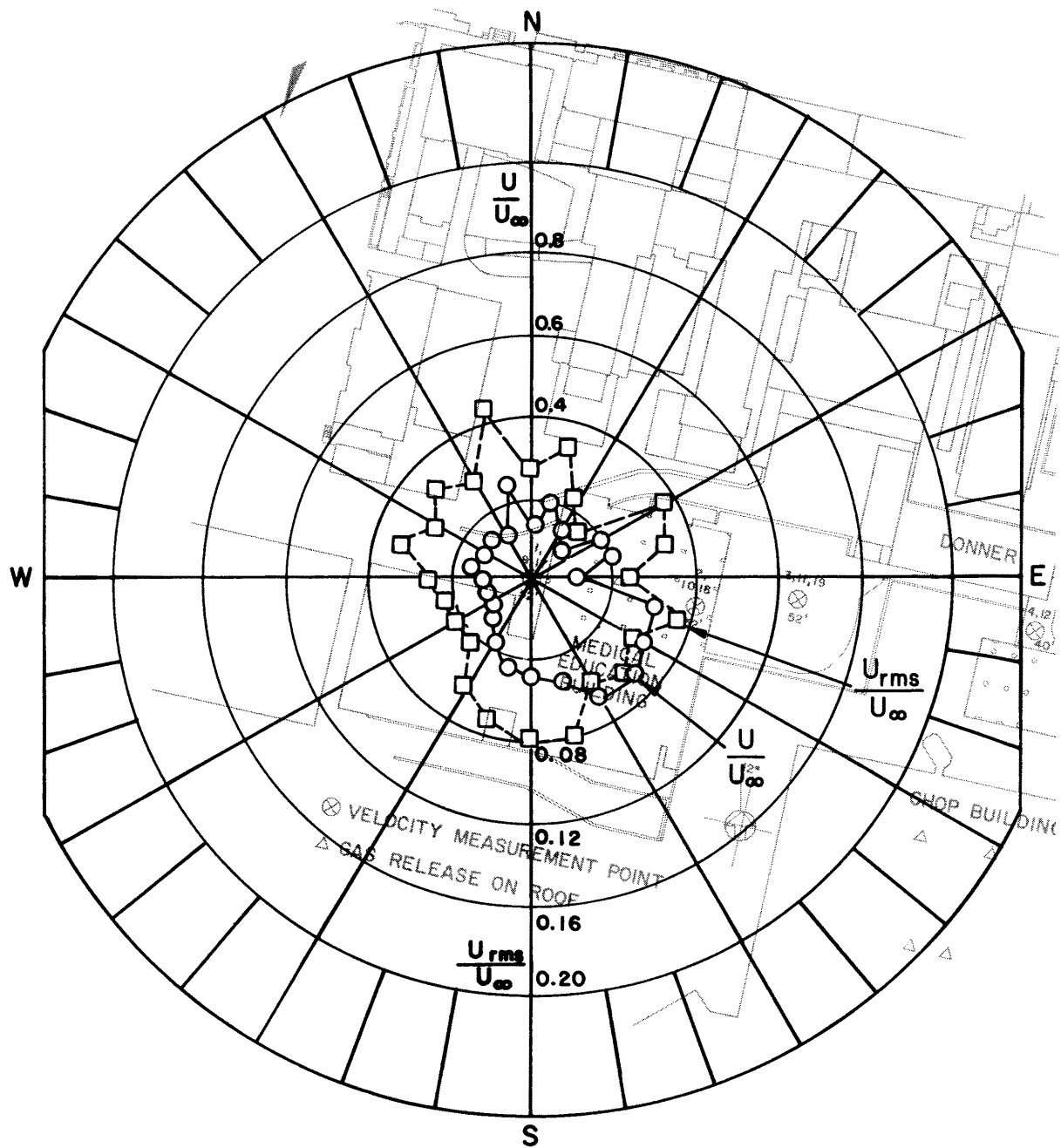


Figure 26. Mean Velocity and Turbulence Intensity at Point 17.

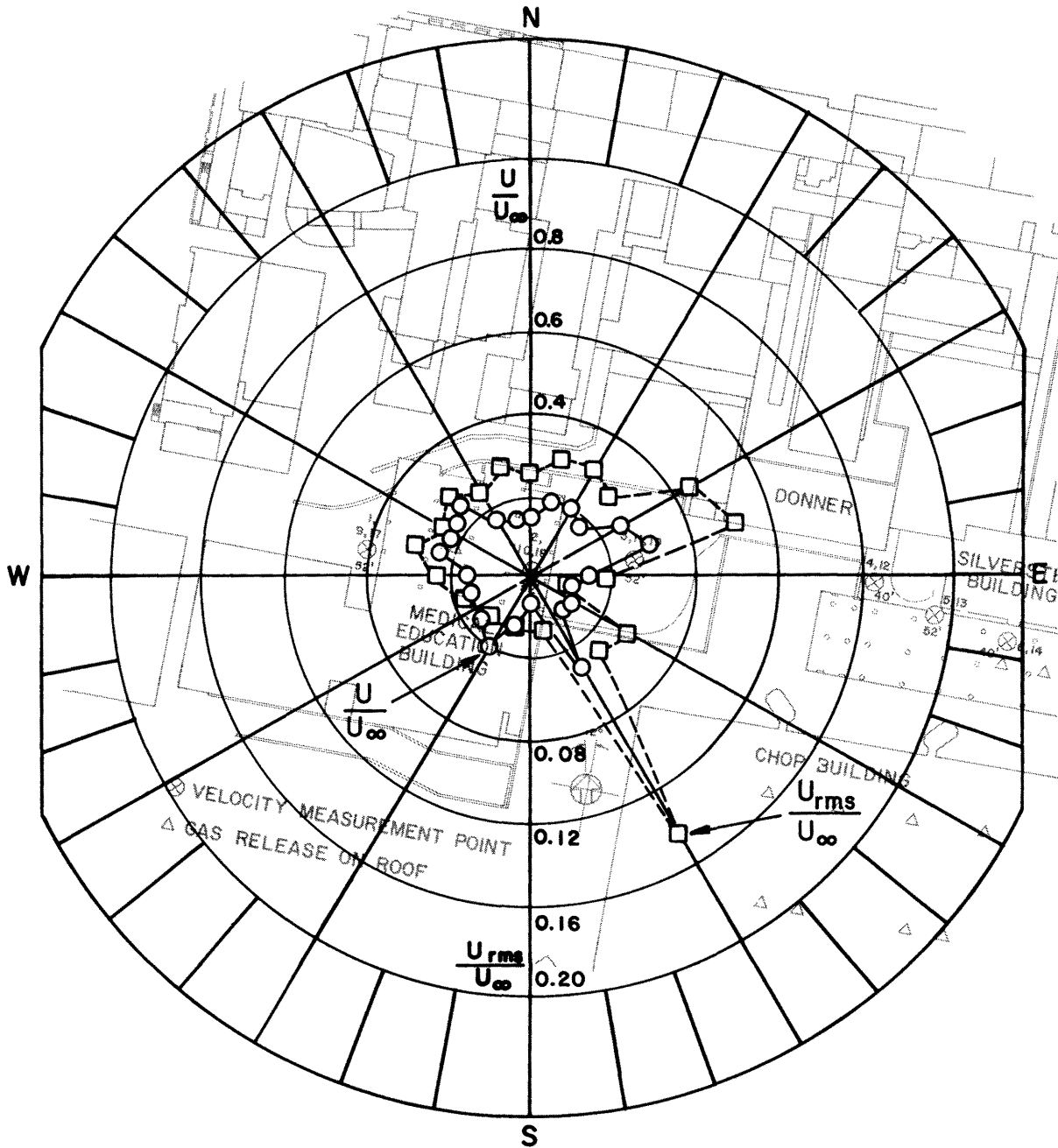


Figure 27. Mean Velocity and Turbulence Intensity at Point 18.

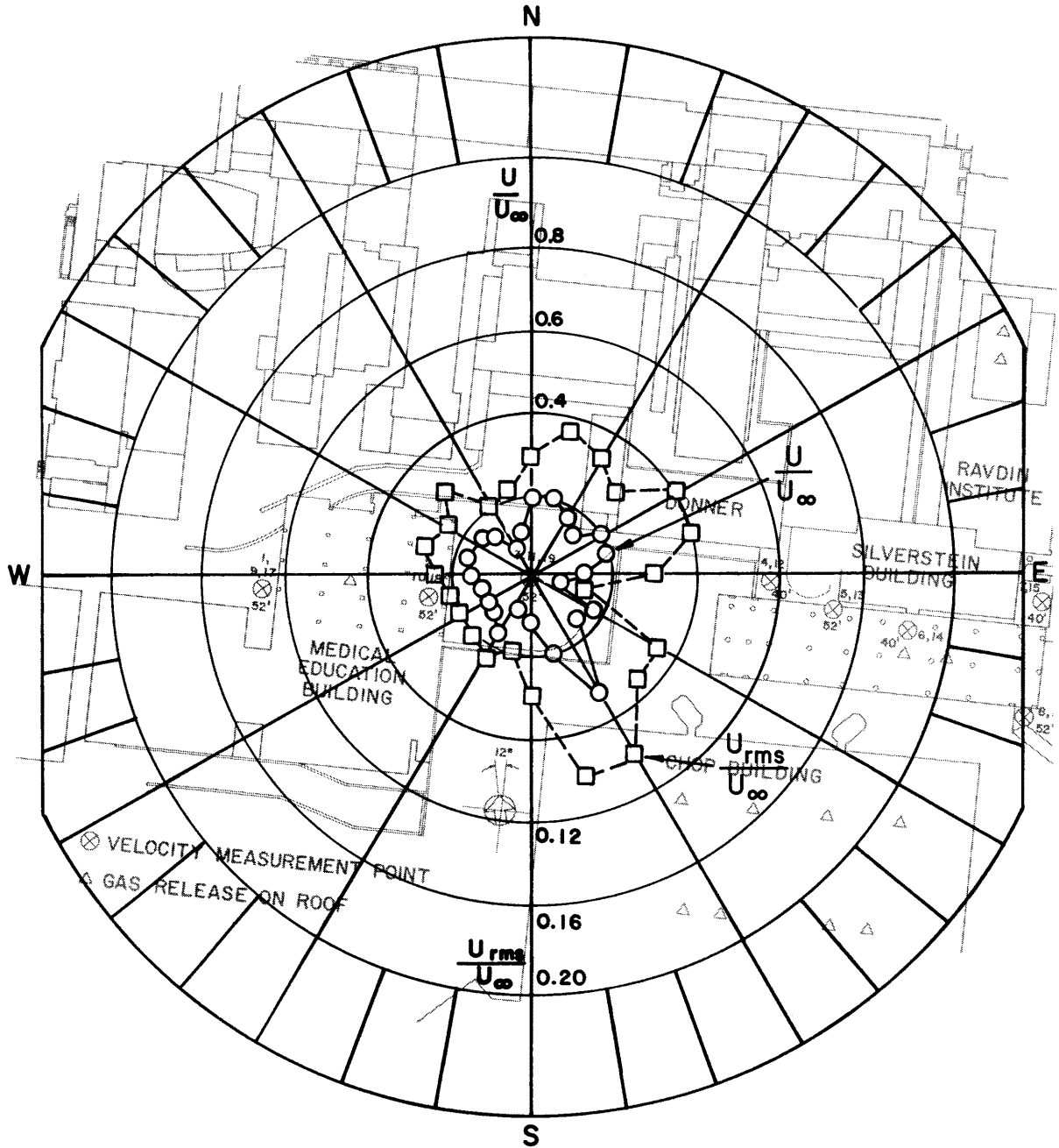


Figure 28. Mean Velocity and Turbulence Intensity at Point 19.